Ultraviolet properties of $\mathcal{N} = 8$ supergravity at five loops

Zvi Bern,[1] John Joseph Carrasco,[2] Wei-Ming Chen,[1] Alex Edison,[1] Henrik Johansson,[3,4]
Julio Parra-Martinez,[1] Radu Roiban,[5] and Mao Zeng[1]

[1]Mani L. Bhaumik Institute for Theoretical Physics, Department of Physics and Astronomy,
University of California at Los Angeles, Los Angeles, California 90095, USA
[2]Institute of Theoretical Physics, Université Paris-Saclay, CEA-Saclay and CNRS,
F-91191 Gif-sur-Yvette cedex, France
[3]Department of Physics and Astronomy, Uppsala University, 75108 Uppsala, Sweden
[4]Nordita, Stockholm University and KTH Royal Institute of Technology,
Roslagstullsbacken 23, 10691 Stockholm, Sweden
[5]Institute for Gravitation and the Cosmos, Pennsylvania State University, University Park,
Pennsylvania 16802, USA

We use the recently developed generalized double-copy construction to obtain an improved representation of the five-loop four-point integrand of $\mathcal{N} = 8$ supergravity whose leading ultraviolet behavior we analyze using state-of-the-art loop-integral expansion and reduction methods. We find that the five-loop critical dimension where ultraviolet divergences first occur is $D_c = 24/5$, corresponding to a $D^8 R^4$ counterterm. This ultraviolet behavior stands in contrast to the cases of four-dimensional $\mathcal{N} = 4$ supergravity at three loops and $\mathcal{N} = 5$ supergravity at four loops whose improved ultraviolet behavior demonstrates enhanced cancellations beyond implications from standard symmetry considerations. We express this $D_c = 24/5$ divergence in terms of two relatively simple positive-definite integrals with vanishing external momenta, excluding any additional ultraviolet cancellations at this loop order. We note nontrivial relations between the integrals describing this leading ultraviolet behavior and integrals describing lower-loop behavior. This observation suggests not only a path towards greatly simplifying future calculations at higher loops, but may even allow us to directly investigate ultraviolet behavior in terms of simplified integrals, avoiding the construction of complete integrands.

I. INTRODUCTION

Since the discovery of supergravity theories [1], a complete understanding of their ultraviolet properties has remained elusive. Despite tremendous progress over the years, many properties of gravitational perturbation theory remain unknown. Power-counting arguments, driven by the dimensionality of Newton's constant, suggest that all pointlike theories of gravity should develop an ultraviolet divergence at a sufficiently high-loop order. However, if a pointlike theory were ultraviolet finite, it would imply the existence of an undiscovered symmetry or structure that should likely have a fundamental impact on our understanding of quantum gravity. Explicit calculations in recent years have revealed the existence of hidden properties, not readily apparent in Lagrangian formulations. One might wonder whether these tame the ultraviolet behavior of

pointlike gravity theories. For example, all-loop-order unitarity cuts exhibit remarkable infrared and ultraviolet cancellations [2] whose consequences remain to be fully explored. Indeed, we know of examples in $\mathcal{N} = 4$ [3] and $\mathcal{N} = 5$ [4] supergravity theories that display "enhanced cancellations" [5–9], where quantum corrections exclude counterterms thought to be consistent with all known symmetries. In addition, there are indications that anomalies in known symmetries of supergravity theories play a role in the appearance of ultraviolet divergences [10,11]. Restoration of these symmetries in S-matrix elements by finite local counterterms may lead to the cancellation of known divergences. In this paper, we take a step forward by presenting a detailed analysis of the ultraviolet behavior of the five-loop four-point scattering amplitude in the maximally supersymmetric theory, $\mathcal{N} = 8$ supergravity[1] [12],

[1]Strictly speaking the maximally supersymmetric theory is only recognized as $\mathcal{N} = 8$ supergravity in four dimensions. While we concern ourselves with mainly higher dimensions, in this paper we take the liberty to apply the four-dimensional nomenclature.

and observe properties that should help us determine its four-dimensional ultraviolet behavior at even higher loops.

Its many symmetries suggest that, among the pointlike theories of gravity, the maximally supersymmetric theory has the softest ultraviolet behavior. These symmetry properties also make it technically easier to explore and understand its structure. Over the years there have been many studies and predictions for the ultraviolet behavior of $\mathcal{N} = 8$ supergravity [13,14]. The current consensus, based on standard symmetry considerations, is that $\mathcal{N} = 8$ supergravity in four dimensions is ultraviolet finite up to at least seven loops [15–17]. Through four loops, direct computation using modern scattering amplitude methods prove that the critical dimension of $\mathcal{N} = 8$ supergravity where divergences first occur is [18–20]

$$D_c = \frac{6}{L} + 4, \qquad (2 \leq L \leq 4) \qquad (1.1)$$

where L is the number of loops. This matches the formula [18,21] for $\mathcal{N} = 4$ super-Yang-Mills theory [22] which is known to be an ultraviolet finite theory in $D = 4$ [23]. At one loop the critical dimension, for both $\mathcal{N} = 4$ super-Yang-Mills theory and $\mathcal{N} = 8$ supergravity [13], is $D_c = 8$. We define the theories in dimensions $D > 4$ via dimensional reduction of $\mathcal{N} = 1$ supergravity in $D = 11$ and $\mathcal{N} = 1$ super-Yang-Mills theory in $D = 10$ [13].

In this paper we address the longstanding question of whether Eq. (1.1) holds for $\mathcal{N} = 8$ supergravity at five loops. Symmetry arguments [16] suggest $D^8 R^4$ as a valid counterterm and that the critical dimension for the five-loop divergence should be $D_c = 24/5$ instead of that suggested by Eq. (1.1), $D_c = 26/5$. (See also Refs. [15,17].) Such arguments, however, cannot ascertain whether quantum corrections actually generate an allowed divergence. Indeed, explicit three-loop calculations in $\mathcal{N} = 4$ supergravity and four-loop calculations in $\mathcal{N} = 5$ supergravity reveal that while counterterms are allowed by all known symmetry considerations, their coefficients vanish [5,6]. These enhanced cancellations are nontrivial and only manifest upon applying Lorentz invariance and a reparametrization invariance to the loop integrals [8]. This implies that the only definitive way to settle the five-loop question is to directly calculate the coefficient of the potential $D^8 R^4$ counterterm in $D = 24/5$, as we do here. This counterterm is of interest because it is the one that would contribute at seven loops if $\mathcal{N} = 8$ supergravity were to diverge in $D = 4$.

Our direct evaluation of the critical dimension of the $\mathcal{N} = 8$ supergravity theory at five loops proves unequivocally that it first diverges in $D_c = 24/5$ and no enhanced cancellations are observed. The fate of $\mathcal{N} = 8$ supergravity in four-dimensions remains to be determined. Even with the powerful advances exploited in this current calculation, direct analysis at seven loops would seem out of

reach. Fortunately the results of our current analysis, when combined with earlier work at lower loops [5,6,11,19,20,24], reveal highly nontrivial constraints on the subloops of integrals describing the leading ultraviolet behavior through five loops. These patterns suggest not only new efficient techniques to directly determine the ultraviolet behavior at ever higher loops, but potentially undiscovered principles governing the ultraviolet consistency. In this work we will describe these observed constraints, leaving their detailed study for the future.

The results of this paper are the culmination of many advances in understanding and computing gauge and gravity scattering amplitudes at high-loop orders. The unitarity method [25,26] has been central to this progress because of the way that it allows on-shell simplifications to be exploited in the construction of new higher-loop amplitudes. We use its incarnation in the maximal-cut (MC) organization [26] to systematically build complete integrands [27,28].

The unitarity method combines naturally with double-copy ideas, including the field-theoretic version of the string-theory Kawai, Lewellen and Tye (KLT) relations between gauge and gravity tree amplitudes [29] and the related Bern, Carrasco and Johansson (BCJ) color-kinematics duality and double-copy construction [30,31]. The double-copy relationship reduces the problem of constructing gravity integrands to that of calculating much simpler gauge-theory ones. For our calculation, a generalization [27] of the double-copy procedure has proven invaluable [28].

The analysis in Ref. [28] finds the first representation of an integrand for the five-loop four-point amplitude of $\mathcal{N} = 8$ supergravity. The high power counting of that representation obstructs the necessary integral reductions needed to extract its ultraviolet behavior. Here we use similar generalized double-copy methods [27] to construct an improved integrand that enormously simplifies the integration. The key is starting with an improved gauge-theory integrand, which we build by constraining a manifest-power-counting ansatz via the method of maximal cuts. The needed unitarity cuts are easily obtained from the gauge-theory integrand of Ref. [32].

The earlier representation of the supergravity integrand, given in Ref. [28], is superficially (though not actually) quartically divergent in the dimension of interest. The new representation shifts these apparent quartic divergences to contributions that only mildly complicate the extraction of the underlying logarithmic divergences. Our construction proceeds as before except for small differences related to avoiding certain spurious singularities. We include the complete gauge and supergravity integrands in plain-text ancillary files [33].

Recent advances in loop integration methods proved essential for solving the challenges posed by the calculation of ultraviolet divergences at five loops. Related issues

appeared in the five-loop QCD beta function calculation, which was completed recently [34]. For supergravity, higher-rank tensors related to the nature of the graviton greatly increase the number of terms while the absence of subdivergences dramatically simplifies the calculation. At high-loop orders the primary method for reducing loop integrals to a basis relies on integration-by-parts (IBP) identities [35,36]. The complexity of such IBP systems tends to increase prohibitively with the loop order and the number of different integral types. Ideas from algebraic geometry provide a path to mitigating this problem by organizing them in a way compatible with unitarity methods [37–40]. We also simplify the problem by organizing the IBP identities in terms of an SL(5) symmetry of the five-loop integrals [8].

The final expression for the leading ultraviolet behavior is incredibly compact, and exposes, in conjunction with previous results [5,6,11,19,20,24], simple and striking patterns. Indeed, analysis of this leading ultraviolet behavior indicates the existence of potentially more powerful methods for making progress at higher loops.

This paper is organized as follows. In Sec. II, we review the generalized double-copy construction, as well as the underlying ideas including BCJ duality and the method of maximal cuts. We also summarize properties of the previously constructed five-loop four-point integrand of Ref. [28]. In Sec. III, we construct new $\mathcal{N} = 4$ super-Yang-Mills and $\mathcal{N} = 8$ supergravity integrands with improved power-counting properties. Then, in Sec. IV we describe our procedure for expanding the integrands for large loop momenta, resulting in integrals with no external momenta, which we refer to as vacuum integrals. In Sec. V, as a warm up to the complete integral reduction described in Sec. VI, we simplify the integration-by-parts system of integrals by assuming that the only contributing integrals after expanding in large loop momenta are those with maximal cuts. The results for the five-loop ultraviolet properties are given in these sections. In Sec. VII, by collecting known results for the leading ultraviolet behavior in terms of vacuum integrals we observe and comment on the intriguing and nontrivial consistency for such integrals between higher and lower loops. We present our conclusions in Sec. VIII.

II. REVIEW

The only known practical means for constructing higher-loop gravity integrands is the double-copy procedure that recycles gauge-theory results into gravity ones. Whenever gauge-theory integrands are available in forms that manifest the BCJ duality between color and kinematics [30,31], the corresponding (super)gravity integrands are obtained by replacing color factors with the kinematic numerators of the same or of another gauge theory. Experience shows that it is sometimes difficult to find such representations of gauge-theory integrands. In some cases this can be overcome by increasing the power count of individual terms

[41], or by introducing nonlocalities in integral coefficients [42]. Another possibility is to find an integrand where BCJ duality holds on every cut, but does not hold with cut conditions removed [43]. Unfortunately, these ideas have not, as yet, led to a BCJ representation of the five-loop four-point integrand of $\mathcal{N} = 4$ super-Yang-Mills theory.

To avoid this difficulty, a generalized version of the BCJ double-copy construction has been developed. Although relying on the existence of BCJ duality at tree level, the generalized double-copy construction does not use any explicit representation of tree- or loop-level amplitudes that satisfies BCJ duality. It instead gives an algorithmic procedure which converts generic gauge-theory integrands into gravity ones [27]. This is used in Ref. [28] to construct an integrand for the five-loop four-point amplitude of $\mathcal{N} = 8$ supergravity.

In this section we give an overview of the ingredients and methods used in the construction of the five-loop integrand. We begin with a brief review of BCJ duality and the maximal-cut method which underlies and organizes the construction, and then proceed to reviewing the generalized double copy and associated formulas. We then summarize features of the previously constructed integrand [28] for the five-loop four-point amplitude of $\mathcal{N} = 8$ supergravity. In Sec. III we use the generalized double copy to find a greatly improved integrand for extracting ultraviolet properties, which we do in subsequent sections.

A. BCJ duality and the double copy

The BCJ duality [30,31] between color and kinematics is a property of on-shell scattering amplitudes which has so far been difficult to discern in a Lagrangian formulation of Yang-Mills field theories [44,45]. Nevertheless various tree-level proofs exist [46].

The first step to construct a duality-satisfying representation of amplitudes is to organize them in terms of graphs with only cubic (trivalent) vertices. This process works for any tree-level amplitude in any D-dimensional gauge theory coupled to matter fields. For the adjoint representation case, an m-point tree-level amplitude may be written as

$$\mathcal{A}_m^{\text{tree}} = g^{m-2} \sum_j \frac{c_j n_j}{\prod_{\alpha_j} p_{\alpha_j}^2}, \qquad (2.1)$$

where the sum is over the $(2m - 5)!!$ distinct tree-level graphs with only cubic vertices. Such graphs are the only ones needed because the contribution of any diagram with quartic or higher-point vertices can be assigned to a graph with only cubic vertices by multiplying and dividing by appropriate propagators. The nontrivial kinematic information is contained in the kinematic numerators n_j; they generically depend on momenta, polarization, and spinors. The color factors c_j are obtained by dressing every vertex in graph j with the group theory structure constant, $\tilde{f}^{abc} = i\sqrt{2} f^{abc} = \text{Tr}([T^a, T^b]T^c)$, where the Hermitian

generators of the gauge group are normalized via $\text{Tr}(T^a T^b) = \delta^{ab}$. The denominator is given by the product of the Feynman propagators of each graph j.

The kinematic numerators of an amplitude in a BCJ representation obey the same algebraic relations as the color factors [20,30,31,47]. The key property is the requirement that all Jacobi identities obeyed by color factors are also obeyed by the kinematic numerators,

$$c_i + c_j + c_k = 0 \Rightarrow n_i + n_j + n_k = 0, \qquad (2.2)$$

where i, j, and k refer to three graphs which are identical except for one internal edge. Figure 1 shows three basic diagrams participating in the Jacobi identity for color or numerator factors. They can be embedded in a higher-point diagram. Furthermore, the kinematic numerators should obey the same antisymmetry under graph vertex flips as the color factors. A duality-satisfying representation of an amplitude can be obtained from a generic one through generalized gauge transformations—shifts of the kinematic numerators,

$$n_i \to n_i + \Delta_i, \qquad (2.3)$$

which are constrained not to change the amplitude. When the duality is manifest, the kinematic Jacobi relations (2.2) express all kinematic numerators in terms of a small set of "master" numerators. While there is a fairly large freedom in choosing them, only the numerators of certain graphs can form such a basis.

Once gauge-theory tree amplitudes have been arranged into a form where the duality is manifest [30,31], we obtain corresponding gravity amplitudes simply by replacing the color factors of one gauge-theory amplitude with the kinematic numerators of another gauge-theory amplitude,

$$c_i \to \tilde{n}_i, \qquad (2.4)$$

as well as readjusting the coupling constants. This replacement gives the double-copy form of a gravity tree amplitude,

$$\mathcal{M}_m^{\text{tree}} = i \left(\frac{\kappa}{2} \right)^{m-2} \sum_j \frac{\tilde{n}_j n_j}{\prod_{\alpha_j} p_{\alpha_j}^2}, \qquad (2.5)$$

where κ is the gravitational coupling and $\tilde{n}_j$ and n_j are the kinematic numerator factors of the two gauge theories.
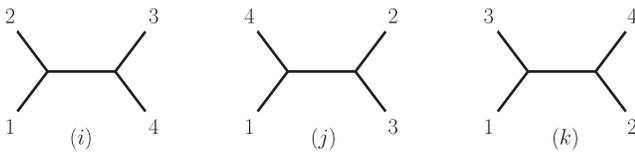
FIG. 1. The three four-point diagrams participating in either color or numerator Jacobi identities.

The gravity amplitudes obtained in this way depend on the specific input gauge theories. As discussed in Refs. [31,44], Eq. (2.5) holds provided that at least one of the two amplitudes satisfies the duality (2.2) manifestly. The other may be in an arbitrary representation.

An earlier related version of the double-copy relation valid at tree level is the KLT relations between gauge and gravity amplitudes [29]. Their general form in terms of a basis of gauge-theory amplitudes is

$$\begin{aligned}
\mathcal{M}_m^{\text{tree}} = i \left(\frac{\kappa}{2} \right)^{m-2} \sum_{\tau, \rho \in \mathcal{S}_{m-3}} K(\tau|\rho) \\
\times \tilde{A}_m^{\text{tree}}(1, \rho_2, \ldots, \rho_{m-2}, m, (m-1)) \\
\times A_m^{\text{tree}}(1, \tau_2, \ldots, \tau_{m-2}, (m-1), m).
\end{aligned} \qquad (2.6)$$

Here the A_m^{tree} are color-ordered tree amplitudes with the indicated ordering of legs and the sum runs over $(m-3)!$ permutations of external legs. The KLT kernel K is a matrix with indices corresponding to the elements of the two orderings of the relevant partial amplitudes. It is also sometimes referred to as the momentum kernel. Compact representations of the KLT kernel are found in Refs. [46,48,49].

At loop level, the duality between color and kinematics (2.2) remains a conjecture [31], although evidence continues to accumulate [20,42,50,51]. As at tree level, loop-level amplitudes in a gauge theory coupled to matter fields in the adjoint representation can be expressed as a sum over diagrams with only cubic (trivalent) vertices:

$$\mathcal{A}_m^{L\text{-loop}} = i^L g^{m-2+2L} \sum_{\mathcal{S}_m} \sum_j \int \prod_{l=1}^L \frac{d^D p_l}{(2\pi)^D} \frac{1}{S_j} \frac{c_j n_j}{\prod_{\alpha_j} p_{\alpha_j}^2}. \qquad (2.7)$$

The first sum runs over the set $\mathcal{S}_m$ of $m!$ permutations of the external legs. The second sum runs over the distinct L-loop m-point graphs with only cubic vertices; as at tree level, by multiplying and dividing by propagators it is trivial to absorb numerators of contact diagrams that contain higher-than-three-point vertices into numerators of diagrams with only cubic vertices. The symmetry factor S_j counts the number of automorphisms of the labeled graph j from both the permutation sum and from any internal automorphism symmetries. This symmetry factor is not included in the kinematic numerator.

The generalization of BCJ duality to loop-level amplitudes amounts to demanding that all diagram numerators obey the same algebraic relations as the color factors [31]. The Jacobi identities are implemented by embedding the three diagrams in Fig. 1 into loop diagrams in all possible ways and demanding that identities of the type in Eq. (2.2) hold for the loop-level numerators as well. In principle, given any representation of an amplitude, one may attempt to construct a duality-satisfying one by modifying the

kinematic numerators through generalized gauge transformations (2.3); however, a more systematic approach is to start with an ansatz exhibiting certain desired properties and impose the kinematic Jacobi relations. As at tree level, when the duality is manifest all kinematic numerators are expressed in terms of those of a small number of "master diagrams" [20,42].

Just like with tree numerators, once gauge-theory numerator factors which satisfy the duality are available, replacing the color factors by the corresponding numerator factors (2.4) yields the double-copy form of gravity loop integrands,

$$\mathcal{M}_m^{L\text{-loop}} = i^{L+1}\left(\frac{\kappa}{2}\right)^{m-2+2L} \sum_{S_m} \sum_j \int \prod_{l=1}^{L} \frac{d^D p_l}{(2\pi)^D} \frac{1}{S_j} \frac{\tilde{n}_j n_j}{\prod_{\alpha_j} p_{\alpha_j}^2},$$

(2.8)

where $\tilde{n}_j$ and n_j are gauge-theory numerator factors. The theories to which the gravity amplitudes belong are dictated by the choice of input gauge theories.

Thus, the double-copy construction reduces the problem of constructing loop integrands in gravitational theories to the problem of finding BCJ representations of gauge-theory amplitudes.[2] Apart from offering a simple means for obtaining loop-level scattering amplitudes in a multitude of (super)gravity theories, the double-copy construction has also been applied to the construction of black-hole and other classical solutions [52] including those potentially relevant to gravitational-wave observations [53], corrections to gravitational potentials [54], and the relation between symmetries of supergravity and gauge theory [55–57]. The duality underlying the double copy has also been identified in a wider class of quantum field and string theories [49,58–62], including those with fundamental representation matter [63]. For recent reviews, see Ref. [47].

When it turns out to be difficult to find a duality-satisfying representation of a gauge-theory amplitude, as in the case for the five-loop four-point amplitude of $\mathcal{N} = 8$ supergravity, an alternative method is available. We use the generalized double-copy procedure [27] that relies only on the existence of duality-consistent properties at tree level. This type of approach may also potentially aid applications of BCJ duality to problems in classical gravity.

B. Method of maximal cuts

The generalized double-copy construction of Refs. [27,28] relies on the interplay between the method of maximal cuts

[26] and tree-level BCJ duality. The maximal-cut method is a refinement of the generalized-unitarity method [25], designed to construct the integrand from the simplest set of generalized-unitarity cuts. In the generalized double-copy approach we apply the maximal-cut method in a constructive way, assigning missing contributions to new higher-vertex contact diagrams as necessary.

In both gauge and gravity theories, the method of maximal cuts [26] constructs multiloop integrands from generalized-unitarity cuts that decompose loop integrands into products of tree amplitudes,

$$\mathcal{C}^{N^k MC} = \sum_{\text{states}} \mathcal{A}_{m(1)}^{\text{tree}} \cdots \mathcal{A}_{m(p)}^{\text{tree}}, \quad k \equiv \sum_{i=1}^{p} m(i) - 3p, \quad (2.9)$$

where the $\mathcal{A}_{m(i)}^{\text{tree}}$ are tree-level $m(i)$-multiplicity amplitudes corresponding to the blobs illustrated for various five-loop examples in Figs. 2 and 3. We organize these cuts according to levels that correspond to the number k of internal propagators that remain off shell.

When constructing gauge-theory amplitudes, we use tree amplitudes directly as in Eq. (2.9). For $\mathcal{N} = 4$ super-Yang-Mills it is very helpful to use a four-dimensional on-shell superspace [64] to organize the state sums [65]. Some care is needed to ensure that the obtained expressions are valid in D dimensions, either by exploiting cuts whose super-sums are valid in $D \leq 10$ dimensions [21,32] or using six-dimensional helicity [66]. Once we have one version of a gauge-theory integrand, we can avoid reevaluating the state sums to find new representations, simply by using the cuts of the previously constructed integrand instead of Eq. (2.9) to construct target expressions. In the same spirit, for $\mathcal{N} = 8$ supergravity we can always bypass Eq. (2.9) by making use of the KLT tree relations (2.6). The state sums also factorize allowing us to express the $\mathcal{N} = 8$ supergravity cuts directly in terms of color-order $\mathcal{N} = 4$ super-Yang-Mills cuts. (See Sec. 2 of Ref. [28] for further details.)

Figures 2 and 3 give examples of cuts used in the construction of the integrands of five-loop four-point amplitudes. At the MC level, e.g., the first two diagrams of Fig. 2, the maximum number of internal lines are placed on shell and all tree amplitudes appearing in Eq. (2.9) are three-point amplitudes. At the next-to-maximal-cut (NMC) level, e.g., the third and fourth diagrams of Fig. 2, all except one internal line are placed on shell; all tree amplitudes are

---

[2]Through four loops, there exist BCJ representations of $\mathcal{N} = 4$ super-Yang-Mills amplitudes that exhibit the same graph-by-graph power counting as the complete amplitude, i.e., all ultraviolet cancellations are manifest. It is an interesting open problem whether this feature will continue at higher loops.

MC 280   MC 370   NMC 1023   NMC 673
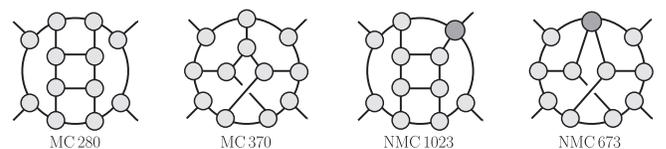
FIG. 2. Sample maximal and next-to-maximal cuts. The exposed lines connecting the blobs are taken to be on-shell delta functions.
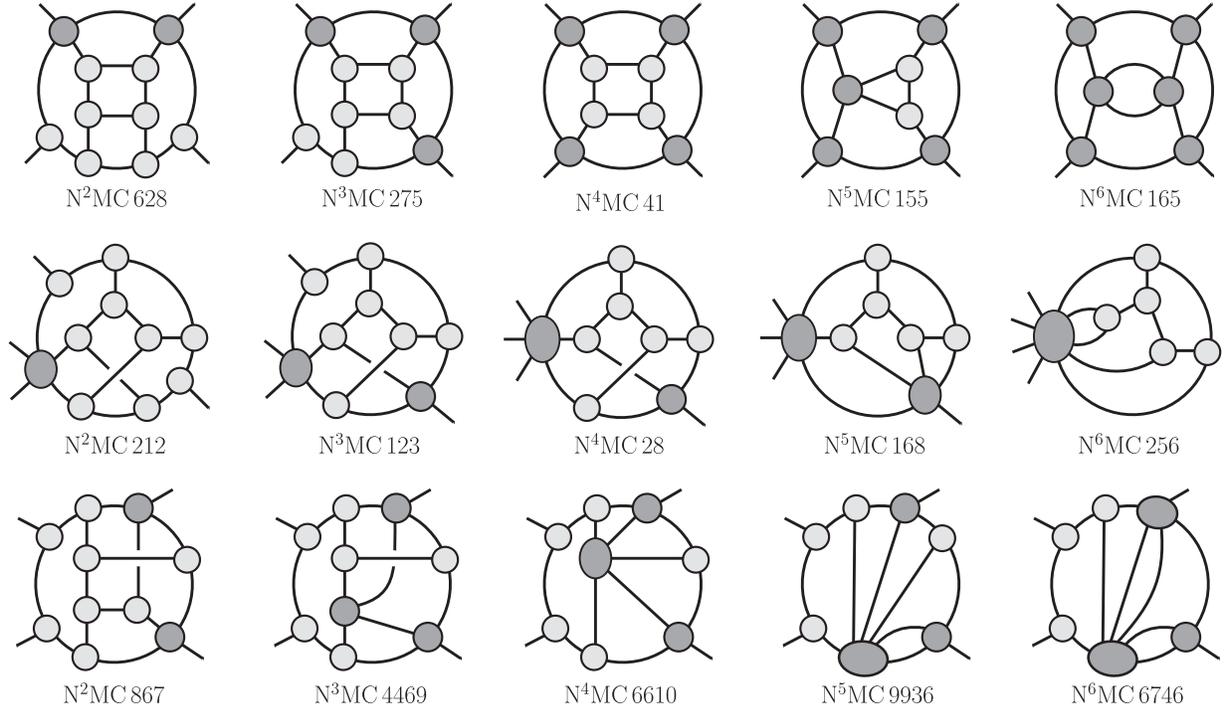
FIG. 3.   Sample N^kMCs used in the construction of five-loop four-point amplitudes. The exposed lines connecting the blobs are taken to be on-shell delta functions.

three-point amplitudes except one which is a four-point amplitude. Similarly, for an N^2MC, two internal lines are kept off shell and so forth, as illustrated in Fig. 3.

In the method of maximal cuts, integrands for loop amplitudes are obtained by first finding an integrand whose maximal cuts reproduce the direct calculation of maximal cuts in terms of sums of products of three-point tree-level amplitudes. This candidate integrand is then corrected by adding to it contact terms such that all NMCs are correctly reproduced and systematically proceeding through the next^k-maximal cuts (N^kMCs), until no further corrections are necessary. The level where this happens is determined by the power counting of the theory and by choices made at earlier levels. For example, for five-loop amplitudes in $\mathcal{N} = 4$ super-Yang-Mills theory, cuts through the N^3MC level are needed, though as we describe in the next section, it is useful to skip certain ill-defined cuts at the N^2MC and N^3MC level and then recover the missing information by including instead certain N^4MC level cuts. For the four-point $\mathcal{N} = 8$ supergravity amplitude at the same loop order, cuts through the N^6MC level are necessary. In general, it is important to evaluate more cuts than the spanning set (necessary for constructing the amplitude) to gain non-trivial crosschecks of the results. For example, in Ref. [28] all N^7MC cuts and many N^8MC cuts were checked, confirming the construction.

To make contact with color/kinematics-satisfying representations of gauge-theory amplitudes it is convenient to absorb all contact terms into diagrams with only cubic vertices [5,6,11,19,20,24,51]. For problems of the complexity of the five-loop supergravity integrand, however, it can be more efficient to assign each new contribution of an N^kMC to a contact diagram instead of to parent diagrams, consisting of ones with only cubic vertices. These new contributions are, by construction, contact terms—they contain only the propagators of the graph with higher-point vertices—because any contribution that can resolve these vertices into propagator terms is already accounted for at earlier levels. In this organization each new contact diagram can be determined independently of other contact diagrams at the same level and depends only on choices made at previous levels. More explicitly, as illustrated in Fig. 4, a new contribution arising from an N^kMC is assigned to a contact diagram obtained from that cut by replacing the blobs representing tree-level amplitudes by vertices with the same multiplicity. The contact terms should be taken off shell by removing the cut conditions in a manner that reflects the diagram symmetry. Off-shell continuation necessarily introduces an ambiguity since it is always possible to include terms proportional to the inverse propagators that vanish by the cut condition; such ambiguities can be absorbed into contact terms at the next cut level.

C. Generalized double-copy construction

Whenever gauge-theory amplitudes are available in a form that obeys the duality between color and kinematics,

FIG. 4. New contribution found via the method of maximal cuts can be assigned to contact terms. The labels (X: Y) correspond to the labeling of Ref. [28] and refer to the level and contact diagram number.

the BCJ double-copy construction provides a straightforward method of obtaining the corresponding (super)gravity amplitudes. If a duality-satisfying representation is expected to exist but is nonetheless unavailable, the generalized double-copy construction supplies the additional information necessary for finding the corresponding (super)gravity amplitude. Below we briefly summarize this procedure. A more thorough discussion can be found in Ref. [28].

The starting point of the construction is a "naive double copy" of two (possibly distinct) gauge-theory amplitudes written in terms of cubic diagrams obtained by applying the double-copy substitution (2.4) to these amplitudes despite none of them manifesting the BCJ duality between color and kinematics. While the resulting expression is not a (super)gravity amplitude, it nonetheless reproduces the maximal and next-to-maximal cuts of the desired (super)gravity amplitude as the three- and four-point tree-level amplitudes entering these cuts obey the duality between color and kinematics. Contact term corrections are necessary to satisfy the N^kMC with $k \geq 2$; the method of maximal cuts can be used to determine them. For N^3 MC and N^3MC at five loops, whose associated contact terms are the most complicated [25,32], it is advantageous to obtain these corrections using formulas that express the cuts in terms of violations of the BCJ relations (2.2).

The existence of BCJ representations at tree level implies that representations should exist for all cuts of gauge-theory amplitudes that decompose the loop integrand into products of tree amplitudes to any loop order. This further suggests that the corresponding cuts of the gravity amplitude can be expressed in double-copy form,

$$\mathcal{C}_{\mathrm{GR}} = \sum_{i_1,\ldots,i_q} \frac{n^{\mathrm{BCJ}}_{i_1,i_2,\ldots i_q} \tilde{n}^{\mathrm{BCJ}}_{i_1,i_2,\ldots i_q}}{D^{(1)}_{i_1} \ldots D^{(q)}_{i_q}}, \qquad (2.10)$$

where the n^{BCJ} and $\tilde{n}^{\mathrm{BCJ}}$ are the BCJ numerators associated with each of the two copies. In this expression the cut conditions are understood as being imposed on the numerators. Each sum runs over the diagrams of each blob and $D^{(m)}_{i_m}$ are the product of the uncut propagators associated to each diagram of blob m. This notation is illustrated in Fig. 5 for an N^2MC. In this figure, each of the two four-point

blobs is expanded into three diagrams, giving a total of nine diagrams. For example, the indices $i_1 = 1$ and $i_2 = 1$ refer to the five-loop diagram produced by taking the first diagram from each blob and connecting it to the remaining parts of the five-loop diagram. The denominators in Eq. (2.10) correspond to the thick (colored) lines in the diagrams.

The BCJ numerators in Eq. (2.10) are related [31,44] to those of an arbitrary representation by a generalized gauge transformation (2.3); the shift parameters follow the same labeling scheme as the numerators themselves,

$$n_{i_1,i_2,\ldots i_q} = n^{\mathrm{BCJ}}_{i_1,i_2,\ldots i_q} + \Delta_{i_1,i_2,\ldots i_q}. \qquad (2.11)$$

The shifts $\Delta_{i_1,i_2,\ldots i_q}$ are constrained to leave the corresponding cuts of the gauge-theory amplitude unchanged. Using such transformations we can reorganize a gravity cut in terms of cuts of a naive double copy and an additional contribution,

$$\mathcal{C}_{\mathrm{GR}} = \sum_{i_1,\ldots,i_q} \frac{n_{i_1,i_2,\ldots i_q} \tilde{n}_{i_1,i_2,\ldots i_q}}{D^{(1)}_{i_1} \ldots D^{(q)}_{i_q}} + \mathcal{E}_{\mathrm{GR}}(\Delta), \qquad (2.12)$$

where the cut conditions are imposed on the numerators. Rather than expressing the correction $\mathcal{E}_{\mathrm{GR}}$ in terms of the generalized-gauge-shift parameters, it is useful to reexpress the correction terms as bilinears in the violations of the kinematic Jacobi relations (2.2) by the generic gauge-theory amplitude numerators. These violations are known as BCJ discrepancy functions.

As an example, the cut in Fig. 5 is composed of two four-point tree amplitudes and the rest are three-point amplitudes. For any cut of this structure, two four-point trees connected to any number of three-point trees, the correction has a simple expression,

$$\mathcal{E}^{4\times 4}_{\mathrm{GR}} = -\frac{1}{d^{(1,1)}_1 d^{(2,1)}_1} \left(J_{\bullet 1,1} \tilde{J}_{1,\bullet 2} + J_{1,\bullet 2} \tilde{J}_{\bullet 1,1} \right), \qquad (2.13)$$

where $d^{(b,p)}_i$ is the pth propagator of the ith diagram inside the bth blob and
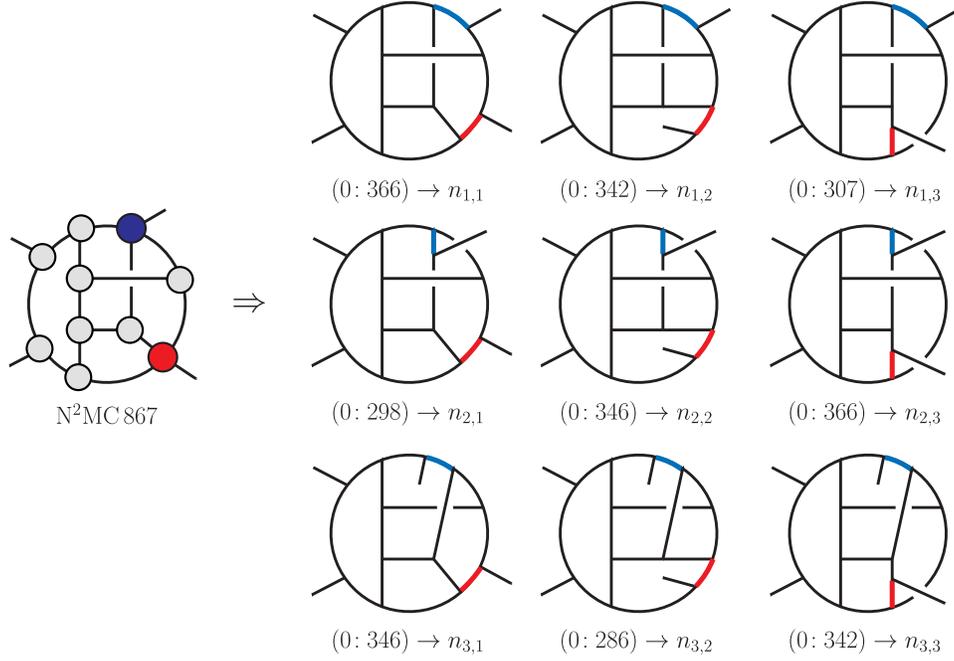
FIG. 5. An example illustrating the notation in Eq. (2.10). Expanding each of the two four-point blobs gives a total of nine diagrams. The label N²MC 867 refers to the 867th diagram of the second level cuts, and the $n_{i,j}$ correspond to labels used in the cut. The shaded thick (blue and red) lines are the propagators around which BCJ discrepancy functions are defined.

$$J_{\bullet,i_2} \equiv \sum_{i_1=1}^{3} n_{i_1 i_2}, \qquad J_{i_1,\bullet} \equiv \sum_{i_2=1}^{3} n_{i_1 i_2},$$

$$\tilde{J}_{\bullet,i_2} \equiv \sum_{i_1=1}^{3} \tilde{n}_{i_1 i_2}, \qquad \tilde{J}_{i_1,\bullet} \equiv \sum_{i_2=1}^{3} \tilde{n}_{i_1 i_2} \qquad (2.14)$$

are BCJ discrepancy functions. Notably, these discrepancy functions vanish whenever the numerators involved satisfy the BCJ relations, even if the representation as a whole does not satisfy them. Such expressions are not unique and can be rearranged using various relations between J s [27,28,67]. For example, an alternative version, equivalent to Eq. (2.13), is

$$\mathcal{E}_{\mathrm{GR}}^{4\times4} = -\frac{1}{9} \sum_{i_1,i_2=1}^{3} \frac{1}{d_{i_1}^{(1,1)} d_{i_2}^{(2,1)}} (J_{\bullet,i_2} \tilde{J}_{i_1,\bullet} + J_{i_1,\bullet} \tilde{J}_{\bullet,i_2}). \quad (2.15)$$

Similarly, a cut with a single five-point tree amplitude and the rest three-point tree amplitudes is given by

$$\mathcal{C}_{\mathrm{GR}}^{5} = \sum_{i=1}^{15} \frac{n_i \tilde{n}_i}{d_i^{(1)} d_i^{(2)}} + \mathcal{E}_{\mathrm{GR}}^{5} \quad \text{with}$$

$$\mathcal{E}_{\mathrm{GR}}^{5} = -\frac{1}{6} \sum_{i=1}^{15} \frac{J_{\{i,1\}} \tilde{J}_{\{i,2\}} + J_{\{i,2\}} \tilde{J}_{\{i,1\}}}{d_i^{(1,1)} d_i^{(1,2)}}, \quad (2.16)$$

where $J_{\{i,1\}}$ and $J_{\{i,2\}}$ are BCJ discrepancy functions associated with the first and second propagator of the ith diagram. (See Ref. [28] for further details.)

As the cut level k increases the formulas relating the amplitudes' cuts with the cuts of the naive double copy become more intricate, but the basic building blocks remain the BCJ discrepancy functions. The formulas often enormously simplify the computation of the contact term corrections and are especially helpful at five loops at the N²MC and N³MC level, where calculating the contact terms via the maximal-cut method can be rather involved. Beyond this level the contact terms become much simpler due to a restricted dependence on loop momenta and are better dealt with using the method of maximal cuts and KLT relations [29], as described in Ref. [28].

D. Previously constructed five-loop four-point integrands

Five-loop four-point integrands have previously been constructed for $\mathcal{N} = 4$ super-Yang-Mills [32] and $\mathcal{N} = 8$ supergravity [28]. Here we review some of their properties which serve as motivation for the construction in Sec. III of new $\mathcal{N} = 4$ super-Yang-Mills and $\mathcal{N} = 8$ supergravity integrands with better manifest ultraviolet properties.

The five-loop four-point integrand of $\mathcal{N} = 8$ supergravity constructed in Ref. [28] is obtained through the generalized double-copy procedure, starting from a slightly modified form of the corresponding $\mathcal{N} = 4$ super-Yang-Mills integrand of Ref. [32]. This modified
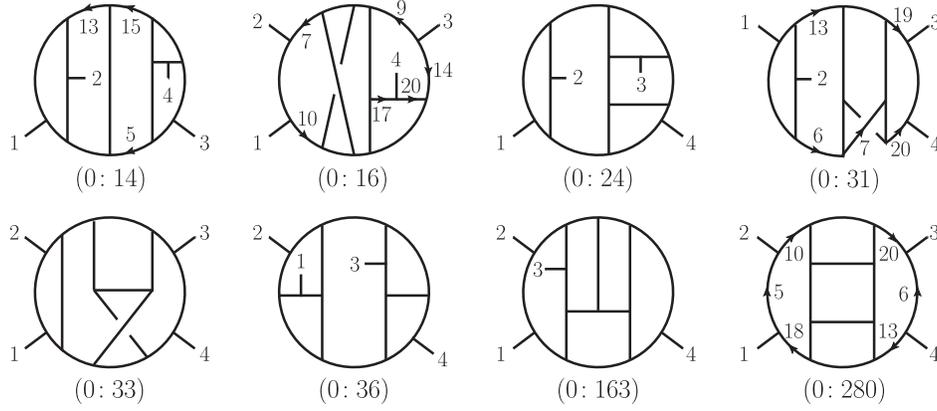
FIG. 6. Sample graphs for the five-loop four-point $\mathcal{N} = 4$ super-Yang-Mills amplitude. The graph labels correspond to the ones in Ref. [28] and here.

super-Yang-Mills representation is given explicitly in an ancillary file of Ref. [28].

All representations of the five-loop four-point $\mathcal{N} = 4$ super-Yang-Mills amplitude that we use contain solely diagrams with only cubic (trivalent) vertices, so can be written using Eq. (2.7) as

$$
\mathcal{A}_4^{(5)} = i g^{12} st A_4^{\text{tree}} \sum_{\mathcal{S}_4} \sum_{i=1}^{N_D} \int \prod_{j=5}^{9} \frac{d^D \ell_j}{(2\pi)^D} \frac{1}{S_i} \frac{c_i N_i}{\prod_{m_i=5}^{20} \ell_{m_i}^2},
$$
(2.17)

where we have explicitly extracted an overall crossing symmetric prefactor of $st A_4^{\text{tree}}$ from the kinematic numerators when compared to Eq. (2.7). The gauge coupling is g, the color-ordered D-dimensional tree amplitude is $A_4^{\text{tree}} \equiv A_4^{\text{tree}}(1, 2, 3, 4)$, and $s = (k_1 + k_2)^2$

and $t = (k_2 + k_3)^2$ are the standard Mandelstam invariants. We denote external momenta by k_i with $i = 1, \ldots, 4$ and the five independent loop momenta by ℓ_j with $j = 5, \ldots, 9$. The remaining momenta ℓ_j with $10 \leq j \leq 20$ of internal lines are linear combinations of the five independent loop momenta and external momenta. As always, the color factors c_i of all graphs are obtained by dressing every three-vertex in the graph with a factor of $\tilde{f}^{abc}$.

The number N_D of diagrams that we include depends on the particular representation we choose. The form given in Ref. [32] has 416 diagrams, while the one used in Ref. [28] has 410 diagrams. Some sample graphs from this list of 410 diagrams are shown in Fig. 6.

It is useful to inspect some of the numerators associated with the sample diagrams. Choosing as examples diagrams 14, 16, 31 and 280 from the 410 diagram representation of Ref. [28], we have the $\mathcal{N} = 4$ super-Yang-Mills numerators

$$
N_{14} = s \left(s^2 s_{3,5} - \frac{5}{2} \ell_5^2 \ell_{13}^2 \ell_{15}^2 \right),
$$

$$
N_{16} = -s \left(s^3 + s^2 \tau_{3,15} - \frac{3}{2} s \ell_7^2 \ell_{10}^2 + \frac{3}{2} \ell_7^2 \ell_{10}^2 (\tau_{1,15} + \tau_{2,15} + \tau_{4,15} + \ell_9^2 - \ell_{14}^2 - \ell_{17}^2 + \ell_{20}^2) \right),
$$

$$
N_{31} = s \left(s \left(-s^2 - \ell_{13}^2 \ell_{20}^2 + s \left(\tau_{6,19} + \ell_{13}^2 + \frac{1}{2} \ell_{20}^2 \right) + \ell_6^2 (\ell_{20}^2 - \ell_{19}^2) \right) - \frac{1}{2} \ell_6^2 \ell_7^2 \ell_{19}^2 \right),
$$

$$
N_{280} = s^4 + s^3 (\tau_{10,13} + \tau_{18,20}) + \frac{1}{2} s^2 (\tau_{10,13}^2 + \tau_{18,20}^2) + 2t (\ell_5^2 + \ell_6^2)(\ell_{13}^2 \ell_{18}^2 + \ell_{10}^2 \ell_{20}^2),
$$
(2.18)

where s and t are the usual Mandelstam invariants and

$$
s_{i,j} = (\ell_i + \ell_j)^2, \qquad \tau_{i,j} = 2 \ell_i \cdot \ell_j. \quad (2.19)
$$

The corresponding naive double-copy numerators are obtained by simply squaring these expressions.

The $\mathcal{N} = 8$ integrand found in Ref. [28] suffers from poor graph-by-graph power counting, which obstructs the

extraction of its leading ultraviolet behavior. Many of its diagrams in the naive double-copy part contain spurious quartic power divergences in $D = 24/5$, which are equivalent to logarithmic divergences in $D = 4$. As discussed in [15–17], such divergences are spurious and should cancel out. The difficulties raised by the spurious power counting are twofold. First, we will see in Sec. IV that their presence causes a rapid growth in the number of terms in the series

expansion of the integrand necessary to isolate the potential logarithmic divergence in $D = 24/5$. Second, this expansion yields graphs with propagators raised to a high power, which leads to an IBP system with billions of integrals.

There are two distinct ways to overcome these difficulties. The first is to construct a new super-Yang-Mills integrand which improves the power counting of the naive double copy. This in turn minimizes the number of integrals and equations in the full IBP system. We will give the construction of this new representation of the $\mathcal{N} = 4$ super-Yang-Mills integrand as well as of the $\mathcal{N} = 8$ supergravity integrand that follows from it in the next section. This represents a complete solution. Still it is useful to have a separate check. Our second resolution is to make simplifying assumptions on the type of integrals that can contribute to the final result after applying IBP integral identities. This approach will be discussed in Sec. V and will allow us to integrate the more complicated integrand of Ref. [28]. The agreement between the results of these two approaches represents a highly nontrivial confirmation of both the integrands and the integration procedure.

III. IMPROVED INTEGRANDS

In this section we describe the construction of a new form of the five-loop four-point integrand for $\mathcal{N} = 4$ super-Yang-Mills theory and then use it to construct an improved $\mathcal{N} = 8$ supergravity integrand. The $\mathcal{N} = 8$ integrand we obtain still exhibits power divergences in $D = 24/5$ but, as we shall see, their structure is such that they do not lead to a dramatic increase in the number of integrals needed for the extraction of the leading logarithmic ultraviolet behavior of the amplitude. In Sec. VI we extract the ultraviolet properties using this improved $\mathcal{N} = 8$ five-loop integrand without making any assumptions on the final form of the large-loop momentum integrals.

A. Construction of improved $\mathcal{N} = 4$ super-Yang-Mills integrand

The key power-counting requirement we demand of every term of the improved Yang-Mills representation is that its naive double copy, as described in Sec. II, has no worse than a logarithmic divergence in $D = 24/5$. This translates to a representation with no more than four powers of loop momenta in the kinematic numerator of any one-particle-irreducible diagram. These conditions require us to introduce new diagrams of the type illustrated in Fig. 7. These graphs are characterized by the vanishing of their maximal cuts. For these diagrams, this implies that the poles due to the propagators independent of loop momenta (to which we will refer to as "dangling trees") are spurious. It also turns out that their numerators have fewer than 4 powers of loop momenta. Such dangling tree diagrams are crucial for obtaining ultraviolet-improved supergravity expressions via the generalized double-copy procedure.

The general pattern is that, to improve the double-copy expression, the terms with the highest power counting in the super-Yang-Mills integrand should come from diagrams with dangling trees. Due to the reduced number of possible loop-momentum factors in their kinematic numerators, the squaring of the numerator (naive double copy) of such diagrams keeps the superficial power counting under control.

To construct such a representation of the five-loop four-point $\mathcal{N} = 4$ super-Yang-Mills integrand we apply the maximal-cut method to an ansatz that has the desired power-counting properties. Inspired by the structure of the lower-loop amplitudes [18,20,31,68] we further simplify the ansatz and improve the power-counting properties of the naive double copy by imposing the following constraints:

  (i) Each numerator is a polynomial of degree eight in momenta, of which no more than four can be loop momenta.

 (ii) Every term in every numerator contains at least one factor of an external kinematic invariant, s or t.

(iii) No diagram contains a one-loop tadpole, bubble or triangle subdiagram. Also, two-point two-loop and three-loop subdiagrams, and three-point two-loop subdiagrams, are excluded.

(iv) For each one-loop n-gon the maximum power of the corresponding loop momentum is $n - 4$. In particular, this means that numerators do not depend on the loop momenta of any box subdiagrams.

 (v) Diagram numerators respect the diagram symmetries.

(vi) The external state dependence is included via an overall factor of the tree amplitude.

Such simplifying conditions can always be imposed as long as the system of equations resulting from matching the cuts of the ansatz with those of the amplitude still has solutions. The conditions above turn out to be incompatible with a representation where BCJ duality holds globally on the fully off-shell integrand. They are nevertheless compatible with all two-term kinematic Jacobi relations [meaning where one of the three numerators of the Jacobi relation (2.2) vanishes by the above constraints], which we impose *a posteriori*:

  (i) The solution to cut conditions is such that the ansatz obeys all two-term kinematic Jacobi relations.

Similarly with the earlier representation of the five-loop four-point $\mathcal{N} = 4$ super-Yang-Mills amplitude, we organize the integrand in terms of diagrams with only cubic vertices; the numerators have the structure shown in Eq. (2.17). In the present case we have 752 diagrams. The first 410 diagrams are the same as for the previous integrand [28], some of which are displayed in Fig. 6. There are an additional 342 diagrams, a few of which are displayed in Fig. 7. In addition to the dangling tree graphs discussed above, this includes other diagrams such the ones on the first line of Fig. 7.
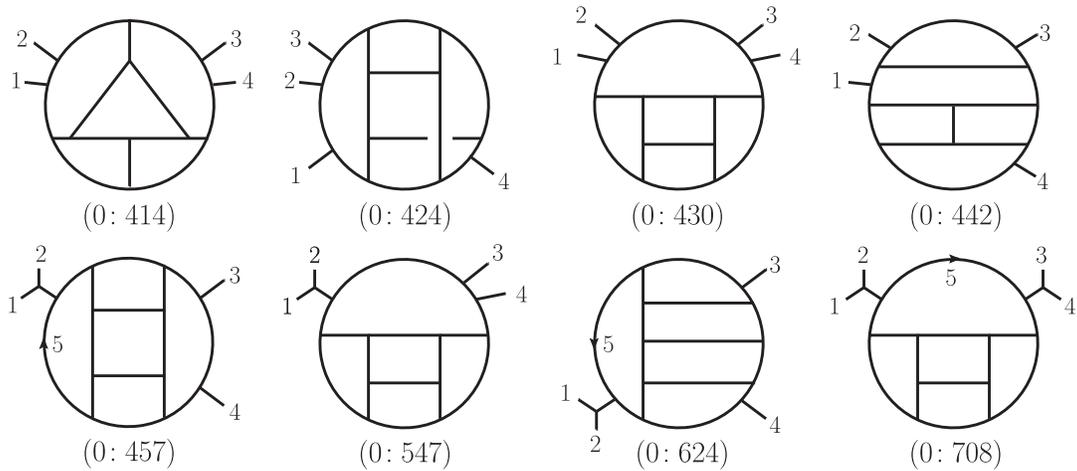
FIG. 7. Some of the additional graphs for the improved representation of the integrand of the five-loop four-point $\mathcal{N} = 4$ super-Yang-Mills amplitude. These graphs were not needed in earlier constructions [28,32]. The labeling scheme is to the contact level and then the diagram number corresponding to the labels of the ancillary files [33].

For each diagram we write down an ansatz for the N_i which is a polynomial of fourth degree in the independent kinematic invariants, subject to the constraints above. Each independent term is assigned an arbitrary parameter. This ansatz is valid for all external states, as encoded in the overall tree-level amplitude factor in Eq. (2.17). This simple dependence on external states is expected only for the four-point amplitudes.[3] The most general ansatz that obeys the first four constraints above has 537,226 terms; requiring that each numerator respects the graph's symmetries and also imposing the maximal cuts of the amplitude reduces this to a more manageable size.

The parameters of the ansatz are determined via the method of maximal cuts. Rather than constructing unitarity cuts directly from their definition as products of tree-level amplitudes, it is far more convenient to use the previously constructed versions [28,32] of the amplitude integrand as input. This approach circumvents the need for supersymmetric state sums [65] (which become nontrivial at high-loop orders and in arbitrary dimensions) and recycles the simplifications which have already been carried out for the construction of that integrand. Moreover, it makes full use of the D-dimensional validity of that integrand, which is confirmed in Ref. [32].

The maximal cuts impose simple constraints on the free parameters; it is convenient to replace them in the ansatz. Next, NMC conditions are solved; as their solution is quite involved, it is impractical to plug it back directly into the ansatz. To proceed, we introduce the notion of a presolution of a given N^kMC as the solution of all constraints imposed by all lower-level cuts which overlap with the given cut. The advantage of using presolutions is that they account for

a large part of the lower-level cut constraints on the parameters entering the given cut without the complications ensuing from simultaneously solving all the lower-level cut conditions and replacing the solution in the ansatz. Thus, instead of simultaneously solving all the NMC cut constraints and evaluating the ansatz on the solution before proceeding to the N^2MC cuts, we construct all the N^2MC presolutions and then solve each of them simultaneously with the N^2MC cut condition. We proceed recursively in this way through all relevant cut levels. The integrand of the amplitude is then found by simultaneously solving all the new constraints on the parameters of the ansatz derived at each level. While this is equivalent to adding contact terms, the ansatz approach effectively distributes them in the diagrams of the ansatz and prevents the appearance of any terms with artificially high power count.

In carrying out this application of the method of maximal cuts we encounter a technical complication with diagrams with four-loop bubble subdiagrams, three of which are illustrated in Fig. 7: (0: 430), (0: 547) and (0: 708). The main difficulty stems from the fact that both propagators connecting the bubble to the rest of the diagram carry the same momentum so the diagram effectively exhibits a doubled propagator. While such double propagators are spurious and can in principle be algebraically eliminated since the representations of Refs. [28,32] do not have them, they nevertheless make difficult the evaluation of the cuts. It moreover turns out that, with our strict power-counting requirements, there is no solution that explicitly eliminates the double poles from all diagrams, even though they cancel in all cuts. Such graphs cause certain cuts to be ill-defined without an additional prescription. Indeed, if only one of the two equal-momentum propagators is cut the tree amplitude containing the second one becomes singular unless a specific order of limits is taken. This phenomenon

---

[3]For higher-point amplitudes the necessary ansatz is more involved [42] and it will not exhibit a clean separation between external state data and loop kinematics.
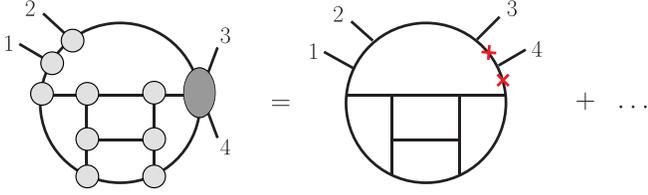
FIG. 8.   This cut is not considered as it contains a singular diagram; instead we recover the missing information from higher level cuts. The shaded (red) "×" marks complete propagators (not replaced by delta functions), the other exposed propagators are all placed on shell (replaced by delta functions).

is illustrated in Fig. 8; by replacing the propagator on one side of the bubble subdiagram with an on-shell delta function, the propagator on the other side, marked by a shaded (red) ×, becomes singular.

One can devise a prescription that realizes the expected cancellation of such $1/0$ terms among themselves. It is, however, more convenient to simply skip the singular cuts altogether and recover the missing information from higher-level cuts that overlap with the skipped ones (i.e., cuts in which the doubled propagator is not cut). In the absence of doubled propagators, cuts through N^3MC level contain all the information necessary for the construction of the amplitude, as seen in [28], because the power counting of the theory implies that numerators can have at most three inverse propagators and thus there can be at most N^3 contact terms. In our case, to recover cut constraints absent due to the unevaluated singular cuts we must include certain N^4MC cuts; the complete list is shown in Fig. 9. All other N^4MC as well as some N^5MC cuts serve as consistency checks of our construction.

Our new representation for the five-loop four-point integrand is given in an ancillary file [33]. Generalized gauge invariance implies that there is no unique form of the integrand; indeed, the global solution of the cut conditions and of the two-term Jacobi relations leaves 10 607 free parameters. They "move" terms between diagrams without affecting any of the unitarity cuts. These parameters should not affect any observable; in particular, they should drop out of the gravity amplitude (after nontrivial algebra) resulting from the generalized double-copy construction based on this amplitude. To simplify the expressions we set them to zero.

It is instructive to see how the power counting of the new representation differs from that of the previous one [28]. Setting the free parameters to zero, the counterparts of the numerators N_{14}, N_{16}, N_{31} and N_{280} shown for the previous representation in Eq. (2.18) are

$$N_{14} = \frac{1}{2} s^3 (\tau_{3,5} - \tau_{4,5} - s),$$

$$N_{16} = N_{14},$$

$$N_{31} = \frac{1}{2} s^3 (\tau_{1,5} + \tau_{1,6} + \tau_{2,5} + \tau_{2,6} + 2\tau_{3,6} + 2\tau_{5,6} - s),$$

$$N_{280} = s^4 + 2s^3 u - u\tau_{2,5}\tau_{3,5}\ell_6^2 + s\tau_{3,5}^2\ell_6^2 + \cdots + 8u^2\ell_5^2\ell_6^2,$$

$$(3.1)$$

where in N_{280} we have kept only a few terms, since it is somewhat lengthy. The complete list of kinematic numerators is contained in the ancillary file [33]. Compared to the super-Yang-Mills numerators in Eq. (2.18), the maximum number of powers of loop momenta dropped from six to one in the first three numerators and to four powers in N_{280}. Consequently, the naive double-copy numerators have only up to eight powers of loop momenta. The naive double-copy numerators also inherit the property that every term carries at least two powers of s or t, a property that all contact term corrections share by construction.

Similarly, the additional diagrams in Fig. 7 also behave very well at large loop momenta. An illustrative sample of the additional numerators is

$$N_{547} = \frac{3}{2} s\ell_5^2 (t\tau_{1,5} - u\tau_{2,5} - 3s\tau_{3,5} - 6u\tau_{3,5}),$$

$$N_{624} = -\frac{61}{10} s^3 (u - t + \tau_{1,5} - \tau_{2,5}),$$

$$N_{708} = 6s^2 (t - u)\ell_5^2, \quad (3.2)$$

where the labels correspond to those in Fig. 7.

The naive double copy of all 752 diagrams gives diagrams that are completely ultraviolet finite in $D = 22/5$. In $D = 24/5$ it exhibits no power divergences, in contrast to the double copy of the earlier representation of the super-Yang-Mills amplitude. As we will see below, the contact term corrections needed to obtain the $\mathcal{N} = 8$ supergravity amplitude will lead to contributions that individually have power

FIG. 9.   The list of additional N^4MCs that are needed to fix the diagrams with doubled propagators.

divergences but, as we will discuss in Sec. IV, it is such that it that does not increase the number of integrals that must be evaluated. Furthermore, as we note in Sec. VI, in $D = 22/5$ the contact term contributions all cancel after IBP reduction, leaving a completely ultraviolet finite result.

To confirm our construction, we have performed the standard checks of verifying cuts beyond those needed for the construction, such as all nonsingular cuts at the N^{4}MC and N^{5}MC levels. We have confirmed that our improved $\mathcal{N} = 4$ super-Yang-Mills integrand generates exactly the same ultraviolet divergence in the critical dimension $D_c = 26/5$ as obtained in Ref. [28] using the earlier representation of the amplitude. To carry out this check we followed the same procedure explained in that paper for extracting the ultraviolet divergence, using the same integral identities.

B. Improved $\mathcal{N} = 8$ supergravity integrand

Armed with the new five-loop four-point integrand of $\mathcal{N} = 4$ super-Yang-Mills theory we now proceed to the construction of the corresponding improved integrand of $\mathcal{N} = 8$ supergravity, following the generalized double-copy construction [27] outlined in Sec. II. Our construction essentially follows the same steps as in Ref. [28], so we will not repeat the details. We obtain a set of contact terms, organized according to levels, which correct the naive double copy to an integrand for the $\mathcal{N} = 8$ supergravity amplitude. As a consequence of the improved term-by-term ultraviolet behavior of the gauge-theory amplitude, the individual terms of the resulting supergravity integrand are also better behaved at large loop momenta.

The difference with the construction in Ref. [28] is related to the existence of the diagrams with doubled propagators in the super-Yang-Mills amplitude, such as (0: 430), (0: 547) and (0: 708) of Fig. 7. Unlike the gauge-theory construction, here we can avoid needing to identify and skip cuts with ill-defined values. To this end we notice that, since the maximal cuts of these diagrams vanish, they contribute only contact terms even in the naive double copy. We may therefore simply set to zero these diagrams in the naive double copy and recover their contributions directly as contact terms at the relevant level. For the same reason we can also set to zero in the naive double copy other diagrams with vanishing maximal cuts. The consistency of this reasoning is checked throughout the calculation by the absence of ill-defined cuts as well as by the locality of all contact term numerators. Had the latter not be the case it would imply the violation of some lower-level cuts. This in turn would have meant that some term we set to zero contributed more than merely contact terms to the amplitude. The net effect is that we can build the complete integrand by using cuts through the N^{6}MC level, just as in the previous construction [28], and there is no need to go beyond this, except to verify the completeness of the result.

As discussed in Sec. II, the cuts of the supergravity amplitude can be computed in terms of the BCJ

discrepancy functions of the full gauge-theory amplitude rather than from the discrepancy functions of the amplitude with the doubled-propagator diagrams set to zero. It turns out that the cuts touching the doubled-propagator diagrams are sufficiently simple to be efficiently evaluated using KLT relations on the cuts. The completeness of the construction is guaranteed by verifying all (generalized) unitarity cuts.

The complete amplitude is given by a sum over the 752 diagrams of the naive double copy and the 85,926 contact term diagrams,

$$
\mathcal{M}_4^{\text{5-loop}} = i \left(\frac{\kappa}{2}\right)^{12} stu M_4^{\text{tree}} \sum_{k=0}^{6} \sum_{\mathcal{S}_4} \sum_{i=1}^{T_k} \int \prod_{j=5}^{9} \frac{d^D \ell_j}{(2\pi)^D}
$$
$$
\times \frac{1}{S_i} \frac{\mathcal{N}_i^{(k)}}{\prod_{m_i=5}^{20-k} \ell_{m_i}^2}, \tag{3.3}
$$

where M_4^{tree} is the four-point $\mathcal{N} = 8$ supergravity tree amplitude and $u = -s - t$. Here T_k is the total number of diagrams at level k; they are given in Table I. The diagram count at each level differs somewhat from the earlier construction [28] because here we include all the daughter diagrams that arise collapsing propagators of any of the 752 parent diagrams of the naive double copy instead of those obtained only from the first 410 diagrams. The parent-level diagrams are obtained from the improved representation of the $\mathcal{N} = 4$ super-Yang-Mills four-point amplitude through the double-copy substitution (2.4) and setting to zero the numerators of the diagrams shown in Fig. 10. The contact terms are generated using the procedures summarized above; examples corresponding to the cuts in Fig. 3 are shown in Fig. 11. We collect the results for all diagrams, numerators $\mathcal{N}_i^{(k)}$ and symmetry factors, S_i, at each level in the plain-text Mathematica-readable ancillary files [33].

A striking property of the supergravity contact terms, which is obvious from Table I, is that most of them vanish. The precise number of vanishing diagrams depends on the particular starting point used in the naive double copy and

TABLE I. The number of diagrams at each contact-diagram level as well as the number of diagrams at each level with nonvanishing numerators.

Level	No. Diagrams	No. Nonvanishing Diagrams
0	752	649
1	2,781	0
2	9,007	1,306
3	17,479	2,457
4	22,931	2,470
5	20,657	1,335
6	13,071	256
total	86,678	8,473
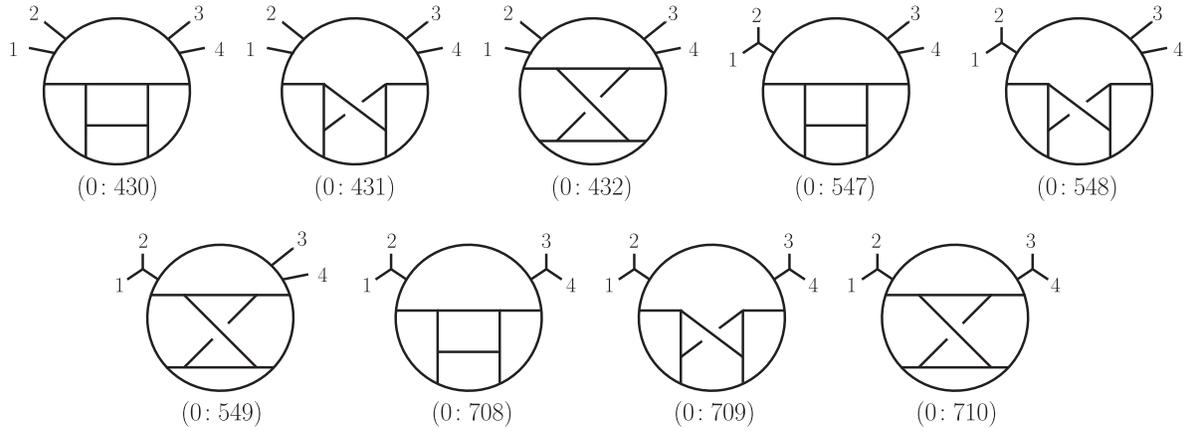
FIG. 10. The diagrams whose numerators were set to zero, to simplify the supergravity construction by avoiding doubled propagators.
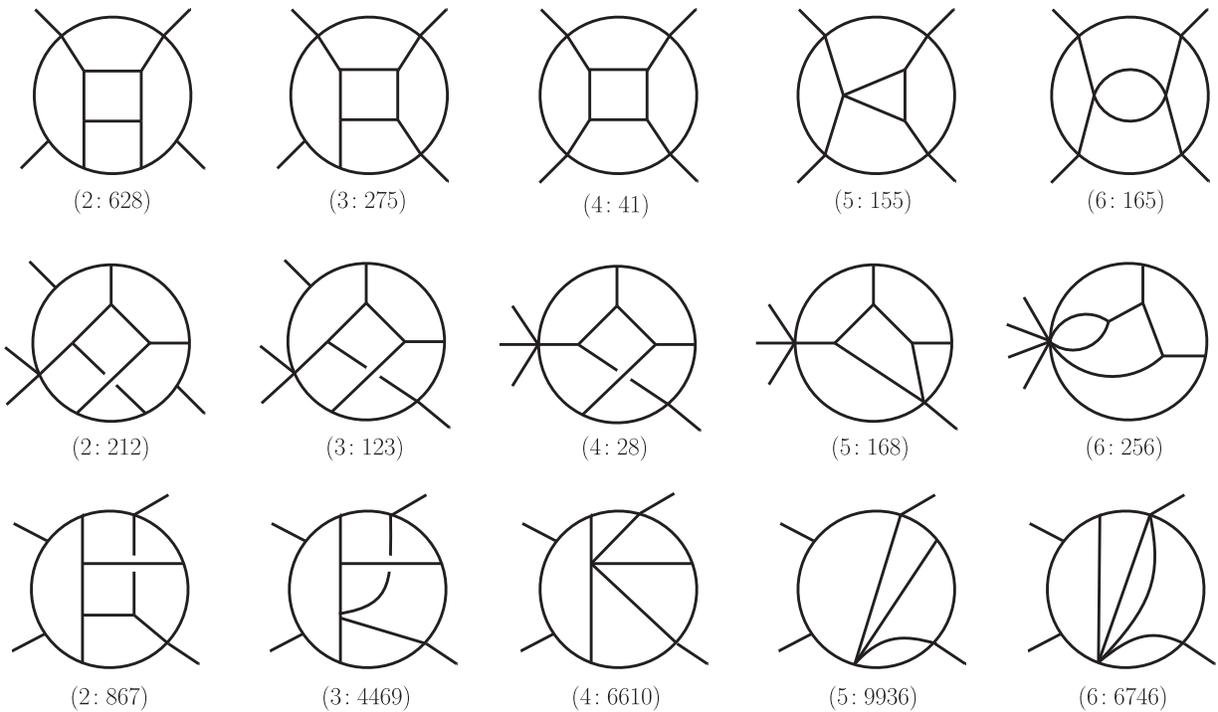
FIG. 11. Sample contact term diagrams corresponding to the cuts in Fig. 3. The labels (X: Y) refer to the level and contact diagram number. The final four diagrams have vanishing numerator; the first eleven are nonvanishing.

on details of the off-shell continuation of the contact terms at each level. As for the previously constructed integrand in Ref. [28], this is a consequence of the many kinematic Jacobi identities that hold for the super-Yang-Mills amplitude used in our construction. This effect is even more clear here, where the $\mathcal{N} = 4$ super-Yang-Mills integrand obeys all the two-term kinematic Jacobi relations. While this integrand does not support a solution for all three-term Jacobi relations, it may be possible to further reduce the number of supergravity contact terms by imposing a judiciously chosen subset of these relations.

IV. ULTRAVIOLET VACUUM INTEGRAL EXPANSION

In previous sections we reviewed the integrand of the five-loop four-point amplitude of $\mathcal{N} = 8$ supergravity found in Ref. [28] and constructed a new one, with certain improved power-counting properties. In this section we expand these integrands in the ultraviolet, i.e., for external momenta small compared to the loop momenta, and point out key features of the new integrand. This expansion generates integrals reminiscent of vacuum integrals with no external momenta; we call such integrals "vacuum

integrals" as well. While we are interested in the logarithmic divergence in $D = 24/5$, both integrands also exhibit spurious quadratic and quartic divergences in this dimension. Finiteness of the five-loop amplitude in $D < 24/5$ guarantees that they should cancel out. However, the graph-by-graph presence of spurious singularities both in the naive double-copy part and in the contact terms of the integrand of Ref. [28] leads to a rapid increase in the number of terms when extracting the logarithmic divergence. By construction, the new integrand can have power divergences only through its contact terms. Moreover, their structure is such that the number of different integrals which appear in the ultraviolet expansion is substantially decreased compared to the earlier integrand.

A. Vacuum expansion of integrands

The basic challenge is to extract logarithmic divergences underneath spurious power divergences. To do so we follow the standard method of series expanding the integrand in the ultraviolet region [69], where the external momenta are much smaller than loop momenta, which are commensurate. This strategy was applied to various supergravity calculations in Refs. [5,6,11,24]. The different orders in this expansion are expressed as vacuum integrals with different degrees of ultraviolet divergence. In dimensional regularization, only logarithmically divergent vacuum integrals can result in a pole. Logarithmically divergent terms in lower dimensions are power divergent in higher dimensions. Thus, by integrating all logarithmically divergent terms in $D < 24/5$, we are checking that power divergences cancel in $D = 24/5$. Indeed, as we explain in Sec. VI, we explicitly verify that in $D = 22/5$ all the divergences cancel. This also proves that any power divergences in $D = 24/5$ are artifacts of our representations. While we do not have representation of the integrand that exhibits only logarithmic divergences in this dimension, the naive double-copy contributions in our new representation were constructed to have this property.

Dimensional analysis shows that the local term[4] in the effective action that corresponds to a logarithmic divergence in $D = 24/5$ at five loops has the generic structure
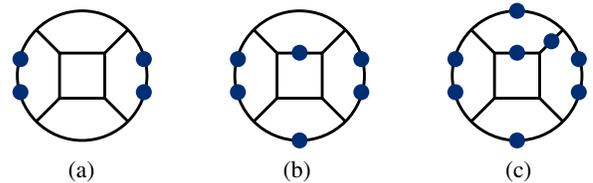
FIG. 12. After series expanding one encounters vacuum diagrams with up to 8 additional propagators, as well as numerators which are suppressed here. Each (blue) dot corresponds to a repeated propagator. Diagrams (a), (b) and (c) are examples with four, six and eight higher-power propagators.

$D^8 R^4$. Its momentum space form has 16 momentum factors; of them, eight correspond to the $(stA^{\text{tree}})^2 = stuM_4^{\text{tree}}$ prefactor of the amplitude. Thus, the logarithmically divergent part of each integral has eight factors of external momenta. Because every term in every supergravity numerator $\mathcal{N}$ has at least two powers of s or t, we need to expand the integrand to at most fourth order in small external momenta.

The dependence of the numerator polynomial on external momenta determines the order to which each term must be expanded. It is therefore useful to decompose each numerator into expressions $\mathcal{N}^{(m)}$ with fixed number m of external momenta (and $16 - m$ powers of loop momentum)

$$\mathcal{N} = \mathcal{N}^{(4)} + \mathcal{N}^{(5)} + \mathcal{N}^{(6)} + \cdots + \mathcal{N}^{(16)}. \quad (4.1)$$

There is freedom in this decomposition, including that induced by the choice of independent loop momenta. Terms with more than eight powers of external momenta in the numerator are ultraviolet finite in $D = 24/5$ and can therefore be ignored. For terms $\mathcal{N}^{(8)}$ with exactly eight powers of external momentum in the numerator we need only the leading terms in the expansion of the propagators as higher-order terms are finite. It suffices therefore to set to zero all external momenta in propagators, e.g., for the $\mathcal{N}^{(8)}$ terms in the diagram shown in Fig. 12(a)

$$\frac{\mathcal{N}^{(8)}}{(\ell_5^2)^3(\ell_6^2)^3\ell_7^2\ell_8^2\ell_9^2(\ell_5 + \ell_7)^2(\ell_5 - \ell_9)^2(\ell_5 + \ell_6 + \ell_7)^2(-\ell_5 - \ell_6 + \ell_9)^2}$$
$$\times \frac{1}{(\ell_5 + \ell_6 + \ell_8 - \ell_9)^2(\ell_5 + \ell_6 + \ell_8)^2(\ell_5 + \ell_6 + \ell_7 + \ell_8)^2}. \quad (4.2)$$

The leading divergence of terms with $4 \leq m \leq 7$ is powerlike. The extraction of the logarithmic divergence underneath requires that propagators be expanded to $(8 - m)$th order in the momenta k_i:

---

[4]This is the same term that may appear at seven loops in $D = 4$, though the appearance of the former of course does not immediately imply the presence of the latter.

$$\frac{\mathcal{N}^{(m)}}{\prod_{i=1}^{I} d_i} \rightarrow \frac{\mathcal{N}^{(m)}}{(8-m)!} \sum_{i_1,\ldots,i_{8-m}=1}^{3} k_{i_1}^{\mu_1} \ldots k_{i_{8-m}}^{\mu_{8-m}} \left(\frac{\partial}{\partial k_{i_1}^{\mu_1}} \cdots \frac{\partial}{\partial k_{i_{8-m}}^{\mu_{8-m}}} \frac{1}{\prod_{i=1}^{I} d_i} \Bigg|_{k_j=0} \right), \tag{4.3}$$

where I is the number of internal lines of the diagram and d_i the corresponding inverse propagators. The action of derivatives leads to propagators raised to higher powers—i.e., to repeated propagators—which we denote by dots, one for each additional power. Up to four further dots appear when derivatives act four times and external momenta are set to zero. Examples, with numerators suppressed, are included in diagrams (b) and (c) of Fig. 12. The increase in the number of classes of vacuum integrals (as specified by the number of dots) leads in turn to an increase in the complexity of the IBP system necessary to reduce them to master integrals. The expansion also leads to higher-rank tensor vacuum integrals, which appear as integrals with numerators containing scalar products of loop and external momenta. We discuss dealing with such integrals below.

It is instructive to contrast, from the standpoint of the vacuum expansion, the old and new four-point five-loop $\mathcal{N} = 8$ supergravity integrands; we will choose the level-0 diagrams 14, 16, 31, 280 shown in Fig. 6 as illustrative examples. The numerators of these diagrams are, respectively, the naive double copies (i.e., squares) of the numerator factors of the old representation of the $\mathcal{N} = 4$ super-Yang-Mills amplitude, given in Eq. (2.18), and the new representation, given in Eq. (3.1). In the old representation, $\mathcal{N}_{0:14}^{(4)}$, $\mathcal{N}_{0:16}^{(4)}$, $\mathcal{N}_{0:31}^{(4)}$, $\mathcal{N}_{0:280}^{(4)}$ are all nonvanishing and, for these terms, the logarithmic divergence is given by Eq. (4.3) with $m = 4$. The resulting vacuum diagrams exhibit up to eight dots.[5] In the improved representation constructed in Sec. III, the first nonvanishing terms in the decomposition of supergravity numerators are $\mathcal{N}_{0:14}^{(8)}$, $\mathcal{N}_{0:16}^{(8)}$, $\mathcal{N}_{0:31}^{(8)}$, $\mathcal{N}_{0:280}^{(8)}$. Thus, no expansion of propagators is needed and the leading term obtained by setting to zero external momenta in the propagators gives the logarithmic divergence in $D = 24/5$. The corresponding vacuum integrals have four dots.

Because of the complexity of the expressions, essentially all combinations of repeated propagators—up to the maximally allowed number of dots—and numerators can appear either in the expansion itself or as part of the IBP system. Thus, a clear requirement to simplify the integration is to reduce the maximal number of dots. As discussed above, we would naively expect up to eight dots from the expansion of the naive double-copy (level-0) diagrams in

the representation of Ref. [28]. It turns out however that, upon reduction of tensor integrals, all seven- and eight-dot vacuum integrals drop out diagram by diagram. This is a consequence of the structure of the representation of the gauge-theory amplitude. As will be seen in Sec. VI, the IBP system does not close unless it includes integrals with an extra dot compared to the desired ones. Thus, for the old representation we need vacuum integrals with up to seven dots. There are 1 292 541 186 different such vacuum integrals of which 16 871 430 are distinct integrals. It is nontrivial to construct and solve the relevant complete IBP system.

For the improved representation of Sec. III, every term in the numerators of level-0 diagrams has at least eight external momenta; thus, the leading term corresponds already to logarithmic divergences in $D = 24/5$. No further expansion of propagators is necessary, implying that the integration of level-0 diagrams in the vacuum expansion requires vacuum integrals with at most four dots and an IBP system relating integrals with up to five dots. This is an enormous simplification over the earlier integrand.

Although simpler, the contact diagrams of the new representation of the four-point five-loop $\mathcal{N} = 8$ integrand contain nonvanishing $\mathcal{N}^{(4)}$ numerator components and thus up to quartic power divergences. Extraction of their logarithmic divergences requires therefore an expansion to fourth order. One might therefore expect vacuum graphs with up to eight dots, which would ruin the simplification of the naive double-copy terms. It turns out however that $\mathcal{N}^{(m)}$ with $m \leq 7$ are nonzero only in contact terms in which at least $(8 - m)$ external lines are attached with four- or higher-point vertex. In the absence of any expansion, the vacuum limit of these graphs has only at most $(m - 4)$ dots; expanding to $(8 - m)$th order (4.3) to extract the logarithmic divergence yields therefore at most four dots. To illustrate this phenomenon, consider the toy example

$$\frac{2\ell_5 \cdot k_1}{\ell_5^2(\ell_5 + k_1)^2} = \frac{1}{\ell_5^2} - \frac{1}{(\ell_5 + k_1)^2}, \tag{4.4}$$

which we embed in a term that is logarithmically divergent, i.e., the numerator on the left-hand side is part of the numerator component $\mathcal{N}^{(8)}$ of some graph. As discussed before, such terms require no expansion and yield vacuum graphs with four dots. The terms on the right-hand side mimic the way contact terms are constructed by canceling propagators. Because each numerator on the right-hand side is missing a power of external momentum compared to the left-hand side, it is now of $\mathcal{N}^{(7)}$ type and we need to

---

[5]The leading term in the small momentum expansion is quartically divergent and corresponds to a logarithmic divergence in $D = 4$ which should cancel on general grounds when all contributions are collected.
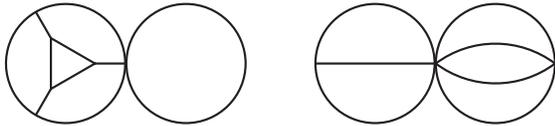
FIG. 13. Sample factorized vacuum integrals that do not contribute because of the absence of subdivergences.

series expand the denominator to first order in external momenta (which may be either k_1 or the other external momenta of the graph). This series expansion produces exactly one doubled propagator. This however it does not increase the number of repeated propagators compared to the left-hand side because in going from the left- to right-hand side we lost a repeated propagator when setting the external momentum k_1 to zero. The net effect is that the total number of dots in any vacuum graphs arising from the expansion of the contact diagrams does not increase beyond the four that arise from naive double-copy diagrams.

Closing the IBP system by including the diagrams with an additional repeated propagator, we obtain 845,323 independent integrals. We will discuss the construction of this system and its solution in Sec. VI.

A further important simplification is that since we are working near a fractional dimension, $D = 24/5 - 2\epsilon$, which in any case is below the critical dimensions at lower-loop orders, no subdivergences are possible. Only genuine five-loop vacuum integrals, which do not factorize into lower-loop integrals, can contribute to the logarithmic ultraviolet divergence. Factorized integrals, such as those shown in Fig. 13, are finite in this dimension and can be ignored.

The result of the expansion in external momenta is a collection of vacuum tensor integrals, in which the numerator factors are polynomials in Mandelstam invariants of external momenta, inverse propagators and scalar products of loop and external momenta. For each integral the numerator is separately homogeneous in the loop and external momentum dependence. These integrals can be further reduced by making use of Lorentz invariance—specifically, that any vacuum tensor integral is a linear combination of products of metric tensors—to separate the dependence on external momenta from that on loop momenta. More precisely, under integration we can replace a two-tensor which is dotted into external momentum by

$$\ell_i^\mu \ell_j^\nu \to \frac{1}{D} \eta^{\mu\nu} \ell_i \cdot \ell_j, \qquad (4.5)$$

and a four-tensor by

$$\ell_i^\mu \ell_j^\nu \ell_k^\rho \ell_l^\sigma \mapsto \frac{1}{D(D-1)(D+2)} \\ \times (A\eta^{\mu\nu}\eta^{\rho\sigma} + B\eta^{\mu\rho}\eta^{\nu\sigma} + C\eta^{\mu\sigma}\eta^{\nu\rho}), \qquad (4.6)$$

where

$$A = (D+1)\ell_i \cdot \ell_j \ell_k \cdot \ell_l - \ell_i \cdot \ell_k \ell_j \cdot \ell_l - \ell_i \cdot \ell_l \ell_j \cdot \ell_k,$$
$$B = -\ell_i \cdot \ell_j \ell_k \cdot \ell_l + (D+1)\ell_i \cdot \ell_k \ell_j \cdot \ell_l - \ell_i \cdot \ell_l \ell_j \cdot \ell_k,$$
$$C = -\ell_i \cdot \ell_j \ell_k \cdot \ell_l - \ell_i \cdot \ell_k \ell_j \cdot \ell_l + (D+1)\ell_i \cdot \ell_l \ell_j \cdot \ell_k.$$
$$(4.7)$$

Since in both cases the highest divergence is quartic, the expansion in small external momenta is to at most fourth order. Thus, there can be at most four scalar products of loop and external momenta and consequently reduction formulas of tensor integrals of rank six or higher are not necessary.

B. Labeling the vacuum diagrams

After applying Lorentz invariance to reduce the expanded integrals to a collection of scalar vacuum integrals, with possible numerators and repeated propagators, we need to organize them into a standard form and eliminate further redundancies. The relevant graph topologies are shown in Fig. 14. A particularly good labeling scheme has been devised by Luthe [70]. Straightforward counting shows that every vacuum integrand in Fig. 14 has 15 independent Lorentz dot products between loop momenta. Depending on the integral, these dot products are either inverse propagators or irreducible numerators i.e., quadratic combinations of loop momenta that are linearly independent of the propagators. Remarkably, a global labeling scheme for momenta can be found for vacuum integrals at five loops. We define, following Ref. [70],

$$q_1 = \ell_1, \quad q_2 = \ell_2, \quad q_3 = \ell_3, \quad q_4 = \ell_4, \quad q_5 = \ell_5,$$
$$q_6 = \ell_1 - \ell_3, \quad q_7 = \ell_1 - \ell_4, \quad q_8 = \ell_1 - \ell_5, \quad q_9 = \ell_2 - \ell_3,$$
$$q_{10} = \ell_2 - \ell_4, \quad q_{11} = \ell_2 - \ell_5, \quad q_{12} = \ell_3 - \ell_5,$$
$$q_{13} = \ell_4 - \ell_5, \quad q_{14} = \ell_1 + \ell_2 - \ell_4, \quad q_{15} = \ell_3 - \ell_4. \qquad (4.8)$$

For example, the labeling of the four parent vacuum integrals—vacuum integrals with only cubic vertices—in this scheme is shown in Fig. 15, where the propagator labeled with i corresponds to q_i^2. The irreducible numerators are q_i^2 for the three i labels missing from that diagram. For daughter diagrams, i.e., the 44 diagrams in Fig. 14 with fewer than 12 distinct propagators, the number of irreducible numerators is larger, so that the total number of independent Lorentz dot products between loop momenta remains the same. For each daughter diagram there are several possible labelings, inherited from its parents. We pick a standard one and map to it all other occurrences of the diagram.

After applying momentum conservation we can rewrite any term in the integrand of a vacuum integral using the 15 invariants. With this labeling scheme we can specify each
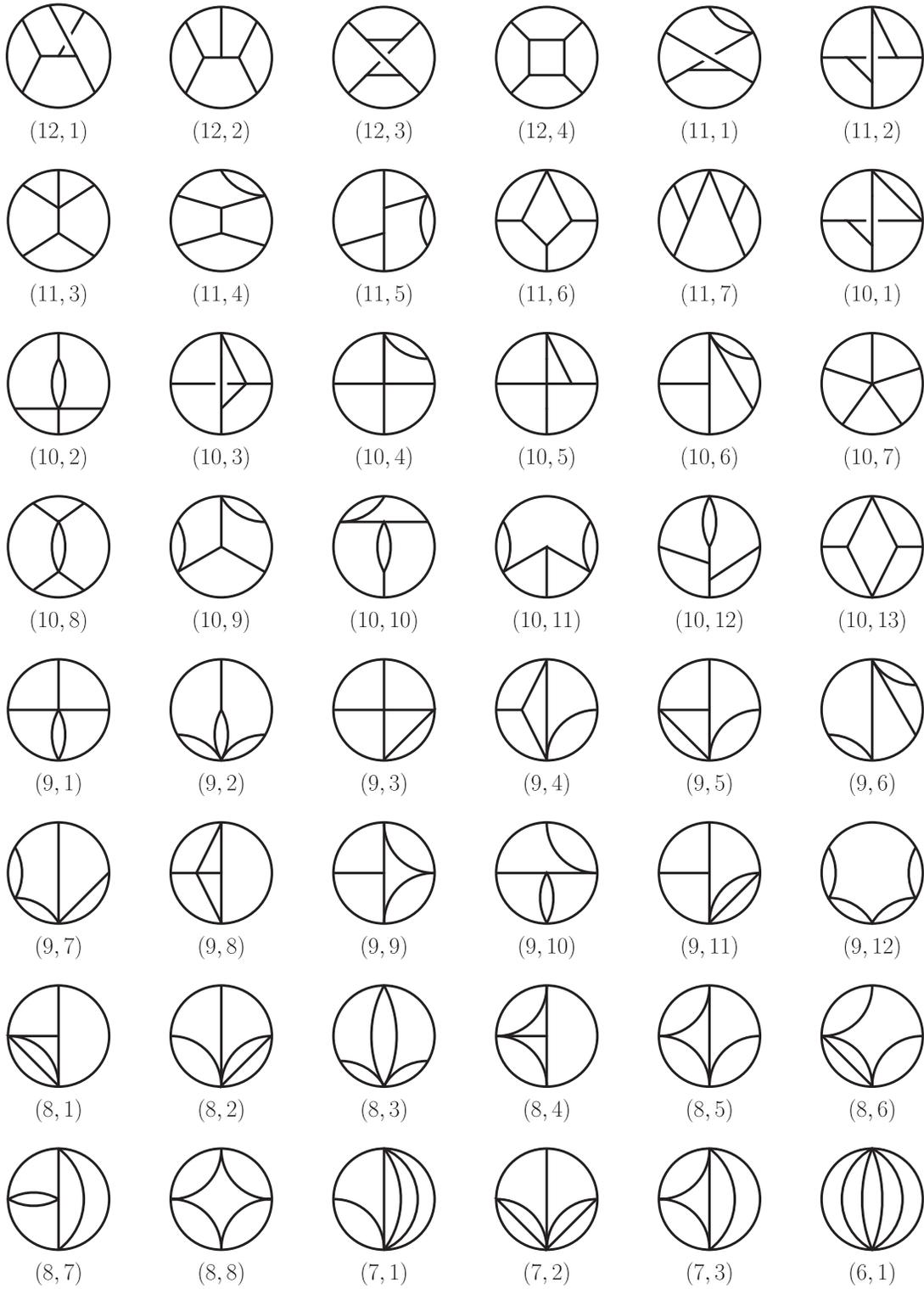
FIG. 14. All 48 independent vacuum propagator structures that do not factorize into products of lower-loop diagrams. The first number in the diagram label is the number of propagators and the second is the diagram number at that level.
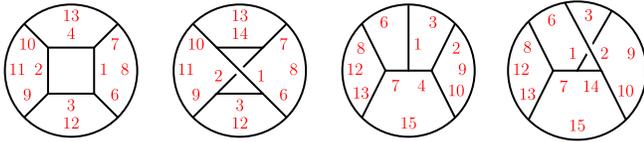
FIG. 15. The parent vacuum integrals—vacuum integrals with only cubic vertices—with 12 distinct propagators and their labels.

integral by a list of the indices representing the exponent of each of the 15 q_i^2,

$$\frac{1}{(q_1^2)^{a_1}(q_2^2)^{a_2}(q_3^2)^{a_3}\cdots(q_{14}^2)^{a_{14}}(q_{15}^2)^{a_{15}}}$$
$$\Leftrightarrow F(a_1, a_2, a_3, \ldots, a_{14}, a_{15}), \qquad (4.9)$$

where a negative power indicates an irreducible numerator rather than a propagator denominator. This description is agnostic to whether the integral is planar or nonplanar, or which diagram the integral is a daughter of. Along with the symmetry relations presented next, it elegantly controls the large redundancies introduced by the vacuum expansion.

In terms of these F s, the four diagrams in Fig. 15 with no irreducible numerators and no repeated propagators are

$$F(1, 1, 1, 1, 0, 1, 1, 1, 1, 1, 1, 1, 1, 0, 0),$$
$$F(1, 1, 1, 0, 0, 1, 1, 1, 1, 1, 1, 1, 1, 1, 0),$$
$$F(1, 1, 1, 1, 0, 1, 1, 1, 1, 1, 0, 1, 1, 0, 1),$$
$$F(1, 1, 1, 0, 0, 1, 1, 1, 1, 1, 0, 1, 1, 1, 1). \qquad (4.10)$$

C. Symmetry relations among vacuum integrals

In order to efficiently express all integrals in terms of a basis it is useful to first eliminate redundant integrals that are identical under relabelings. Figure 16 shows an example of using graph symmetries to rearrange into a canonical format dots that might appear in diagram (12,4), the cube. In terms of the F s, this symmetry maps
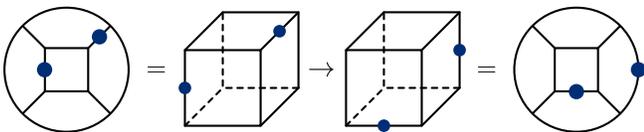
FIG. 16. Moving dots via symmetry in diagram (12,4) corresponding to the cube.
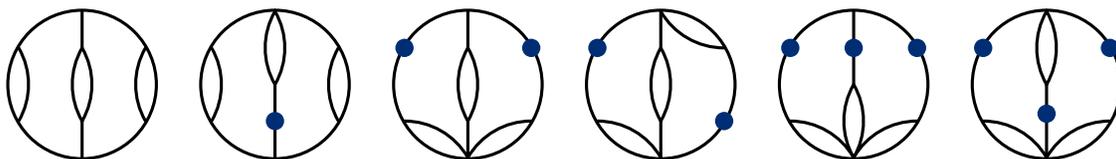
$$F(1, 2, 1, 1, 0, 1, 2, 1, 1, 1, 1, 1, 1, 0, 0)$$
$$\rightarrow F(1, 1, 2, 1, 0, 1, 1, 2, 1, 1, 1, 1, 1, 0, 0). \qquad (4.11)$$

When irreducible numerators are present, the situation is a bit more complex because we also need to map the numerators according to the symmetry transformation. This can generate many contributions when we reexpress the numerators back in terms of the basis q_i^2 monomials. A simple example we encounter is

$$F(1, 1, 1, -1, 0, 3, 2, 0, 0, 0, 0, 2, 2, 1, 0)$$
$$\rightarrow F(3, 1, 1, 0, 0, 0, 0, 2, 1, 1, 0, 2, 0, 1, 0)$$
$$- F(3, 1, 2, -1, 0, 0, 0, 2, 1, 1, 0, 2, 0, 1, 0)$$
$$+ F(3, 1, 2, 0, 0, 0, 0, 2, 1, 1, 0, 2, 0, 1, -1). \qquad (4.12)$$

The vast majority of these numerator relabeling relations often involve iterating the process many times, generating relations between hundreds of different integrals.

Graph isomorphism is not sufficient to remove all the trivial redundancy, since certain nonisomorphic graphs can represent the same Feynman integral. Such relations typically involve "sliding" a bubble subdiagram along the propagators that connect it to the rest of the graph. In addition to a different graph structure, these transformations can change the number of dots, as illustrated in the example in Fig. 17. We implement these nonisomorphism graph relations via a graph transformation that swaps bubble subdiagrams and propagators, corresponding to the swaps which map the diagrams in e.g., Fig. 17 into each other. We will refer to this as "enhanced graph isomorphisms." This method efficiently identifies equivalent five-loop vacuum integrals not related by graph isomorphisms.

A less efficient alternative, which we use in parts of the calculation as a consistency check, is to compute the Symanzik polynomials and bring them to a canonical form [71,72]. This uses analytic properties of Feynman integrals without resorting to their graph representation.

Implementing the isomorphism and nonisomorphism relations, we map all integrals to a set of canonical ones. There are 3 079 716 scalar vacuum integrals with up to five dots and unit numerator, which map onto 94 670 canonical configurations, as demonstrated in Fig. 16.

In the presence of momentum-dependent numerator factors there also exist symmetry relations due to

FIG. 17. Example of nonisomorphic graphs that all correspond to the same Feynman integral.
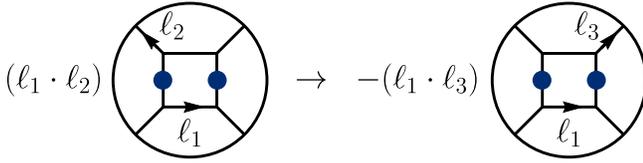
FIG. 18. Numerator relations from residual automorphisms that keep the dot positions invariant.

automorphisms that preserve both the graph structure and the position of the dots but change the numerator. This is distinct from relations of the type in Eq. (4.12) which do not relate canonical integrals, but are used to move dots to canonical positions. An example of one particularly simple such relation is given in Fig. 18. Transformations of this type generate linear relations between canonical integrals, which are similar to IBP relations. Because of this, it is convenient to include and analyze them together with the IBP relations in Sec. VI.

V. SIMPLIFIED ULTRAVIOLET INTEGRATION

In this section we discuss the large-loop-momentum integration of the original form [28] of the five-loop four-point $\mathcal{N} = 8$ supergravity integrand. Although, an assumption will be required, this will not only provide a strong cross-check of the complete result obtained in the next section, but will also point to more powerful ways of extracting the ultraviolet properties of supergravity theories, especially when combined with the observations of Sec. VII. As explained in the previous section, after series expanding and simplifying the original form of the integrand we encounter vacuum integrals with up to six dots, or repeated propagators, and irreducible numerators. Together with the additional dot needed to close the system, this causes a rather unwieldy IBP system. We will see here that the problem can be enormously simplified by targeting parent vacuum integrals—vacuum integrals with only cubic vertices or, equivalently, vacuum integrals that have maximal cuts, or also as vacuum integrals with the maximum number of distinct propagators. The relevant parent vacuum integrals are shown in Fig. 15. We solve the integration-by-parts system on the maximal cuts of the vacuum integrals, using modern algebraic geometry methods that combine unitarity cuts with IBP reduction for Feynman integrals [37–39,73,74].

Besides enormously simplifying reduction to a set of master integrals by focusing on the vacuum integrals with maximal cuts, targeting parent vacuum integrals also has the added benefit of allowing us to immediately drop large classes of contact terms from the integrand, including all contact terms obtained from the N⁵MC and N⁶MC levels, even before expanding into vacuum diagrams. Any term where a propagator is completely canceled in the vacuum graph can be dropped.

In manipulating the vacuum integrals, there are two important issues that must be addressed. The first one is the separation of the infrared and ultraviolet divergences. This is an important ingredient in various studies of ultraviolet properties, such as the analysis of $\mathcal{N} = 4$, $\mathcal{N} = 5$ and $\mathcal{N} = 8$ supergravity at three and four loops [5,6,11,19], and the computation of the five-loop beta function in QCD [34]. Although there are no physical infrared singularities in $D > 4$, our procedure of series expanding around small external momenta introduces spurious ones. We will show in detail in the next section that in an infrared-regularized setup for integrals with no ultraviolet subdivergences, terms in the IBP system that are proportional to the infrared regulator involve only ultraviolet-finite integrals. Thus, since we are interested only in the ultraviolet poles, we can effectively reduce the vacuum integrals without explicitly introducing an infrared regulator. For the rest of this section, when we discuss linear relations between integrals, it should be understood that we actually mean linear relations between the ultraviolet poles of the integrals.

A second issue is that the vacuum expansion of our integrand contains propagators with raised powers, which is in contradiction with the naive unitarity cut procedure of replacing propagators by on-shell delta functions. Fortunately, two solutions to this problem are available in the literature. One option [75] is to define the cut as the contour integral around propagator poles; this effectively identifies the cut as the residue of the propagator pole even for higher-order poles. Another, proposed in Ref. [40], is to use dimension shifting [76] such that all propagators appear only once at the cost of shifting the integration dimension and raising the power of numerators, before imposing the maximal-cut conditions to discard integrals with canceled propagators. Here we will use the second strategy.

Starting with the integrand of Ref. [28], the end result of dimension shifting procedure is a set of vacuum integrals in $D = -36/5 - 2\epsilon$ with a total 30 powers of the irreducible numerators. For example, for the crossed-cube vacuum diagram shown in the second diagram of Fig. 15, we have integrals of the form

$$\int \prod_{k=1}^{5} \frac{d^D \ell_k}{(2\pi)^D} \frac{(q_4^2)^{A_4}(q_5^2)^{A_5}(q_{15}^2)^{A_{15}}}{q_1^2 q_2^2 q_3^2 \hat{q}_4^2 \hat{q}_5^2 q_6^2 q_7^8 q_8^2 q_9^2 q_{10}^2 q_{11}^2 q_{12}^2 q_{13}^2 q_{14}^2 \hat{q}_{15}^2},$$

(5.1)

where $D = -36/5 - 2\epsilon$ and the "hats" in the denominator mean to skip those propagators. The q_i are the uniform momenta defined in Eq. (4.8). Here the three irreducible numerators are q_4^2, q_5^2 and q_{15}^2; these cannot be written as the linear combinations of the 12 propagator denominators, as explained in the previous section. To obtain a logarithmic divergence in the shifted dimension $-36/5$, we need 30 powers of numerator factors

$$A_4 + A_5 + A_{15} = 30, \quad \text{with } A_4 \geq 0, \quad A_5 \geq 0, \quad A_{15} \geq 0. \tag{5.2}$$

In total there are 496 different combinations of A_j that satisfy Eq. (5.2). With the new integrand of Sec. III the power counting is greatly improved so we need only shift to $D = -16/5 - 2\epsilon$ with 20 powers of numerators. This gives 231 integrals to evaluate.

Consider the cross-cube diagram shown in the second diagram in Fig. 15. The IBP identities relating the 496 integrals are of the form

$$\int \prod_k \frac{d^D \ell_k}{(2\pi)^D} \frac{\partial}{\partial \ell_i^\mu} \frac{v_i^\mu}{\prod_j d_j} = 0, \tag{5.3}$$

where v_i^μ has polynomial dependence on external and internal momenta and the d_j are the various propagators. We refer to

$$v_i^\mu \frac{\partial}{\partial \ell_i^\mu}, \tag{5.4}$$

as the IBP-generating vector, while the rest of Eq. (5.3),

$$\int \prod_k \frac{d^D \ell_k}{(2\pi)^D} \frac{1}{\prod_j d_j}, \tag{5.5}$$

is referred to as the seed integral. Integration by parts as above reintroduces auxiliary integrals with propagators raised to higher powers, since the derivatives can act on the propagator denominators. Lowering again the propagator powers through dimension shifting leads still to new integrals because, while of the same topology at the starting ones, they are now in a different dimension.

To eliminate these auxiliary integrals Gluza, Kadja and Kosower [37] formulated IBP relations without doubled propagators, using special IBP-generating vectors that satisfy

$$v_i^\mu \frac{\partial}{\partial \ell_i^\mu} d_j = f_j d_j, \tag{5.6}$$

for *all* values of j with f_j restricted to be polynomials (in external and loop momenta). This cancels any squared propagator generated by derivatives, and does not introduce spurious new denominators since f_j are polynomials. Since the original publication, strategies for solving Eq. (5.6) have been explored in Refs. [37,39,74]. We use the strategy in Ref. [74] to obtain a complete set of vectors v_i^μ using computational algebraic geometry algorithms implemented in SINGULAR [77]. They in turn give the complete set of IBP relations among the 496 cross cube integrals discussed above (5.1), (5.2) and implies that all of them are expressed in terms of a single integral—the second diagram in Fig. 15. A similar analysis solves the analogous problem for the 496 integrals of cube topology and expresses them in terms of the integral corresponding to the first graph in Fig. 15. The IBP systems restricted to integrals with maximal cuts for the parent topologies with internal triangles, corresponding to the third and fourth graph in Fig. 15, sets all integrals to zero, implying that they are all reducible to integrals that do not have maximal cuts.

As a cross-check for the crossed-cube topology, we have also analytically solved for the integrals in closed form by contour integration [73] using the Baikov representations [78], without making use of integral relations of the type (5.3). We refer the reader to Ref. [28] for the details of the analogous computation in $D = 22/5$. In that case, all parent vacuum diagrams cancel, as expected.

By inverting the dimension shifting relations we can reexpress the final result in terms of parent master integral in the original dimension $D = 24/5 - 2\epsilon$. The final result for the leading ultraviolet behavior is remarkably simple:

$$\mathcal{M}_4^{(5)}\Big|_{\text{leading}}^{\text{parent-level}} = -\frac{629}{25}\left(\frac{\kappa}{2}\right)^{12}(s^2 + t^2 + u^2)^2 stu M_4^{\text{tree}}\left(\frac{1}{3}\,\boxminus + \,\boxtimes\right). \tag{5.7}$$

We obtain identical result, whether we start from the integrand of Ref. [28] or the improved one in Sec. III. This provides a highly nontrivial check on the cut construction and the integral reduction procedure. Most importantly, as we show in the next section, the result in Eq. (5.7) is complete, even though we kept only the parent master integrals, which have no canceled propagators. As we shall see in Sec. VII, this seems unlikely to be accidental.

VI. FULL ULTRAVIOLET INTEGRATION

In this section, we extract the ultraviolet divergence of the five-loop four-point $\mathcal{N} = 8$ supergravity amplitude without making any assumptions on the class of vacuum integrals that contribute. To keep the IBP system under control, we use the improved representation of the integrand found in Sec. III, expanded at large loop momentum, as described in Sec. IV. We organize the IBP relations using

and SL(L) reparametrization symmetry of L loop momenta [8]. We also incorporate the integral relations resulting from graph automorphisms that change kinematic numerator factors, a simple example of which is shown in Fig. 18.

A. IBP for ultraviolet poles modulo finite integrals

Since standard IBP reduction is usually performed for full integrals in dimensional regularization, there is a large amount of unnecessary computation for our purpose of

extracting only the ultraviolet poles.[6] We now review setting up a simplified IBP system that only gives linear relations between the leading ultraviolet poles of different vacuum integrals [8].

As a warm up, consider the toy example of two-loop vacuum integrals in $D = 5 - 2\epsilon$ shown in Fig. 19. This example will mimic the supergravity situation because there are no (one-loop) subdivergences due to the properties of dimensional regularization. We define such two-loop integrals as

$$V_{A,B,C} = \int \frac{d^D \ell_1}{(2\pi)^D} \frac{d^D \ell_2}{(2\pi)^D} \frac{1}{[(\ell_1)^2 - m^2]^A [(\ell_2)^2 - m^2]^B [(\ell_1 - \ell_2)^2 - m^2]^C}, \tag{6.1}$$

where we require $A + B + C = 5$ since we are interested in logarithmically divergent integrals. In this case, there are no irreducible numerators.

Consider GL(2) transformations of the loop momenta $\Delta \ell_i \equiv \Omega_{ij} \ell_j$, which generate IBP relations of the form,

$$0 = \int \frac{d^D \ell_1}{(2\pi)^D} \frac{d^D \ell_2}{(2\pi)^D} \frac{\partial}{\partial \ell_i^\mu} \frac{\Omega_{ij} \ell_j^\mu}{[(\ell_1)^2 - m^2]^A [(\ell_2)^2 - m^2]^B [(\ell_1 - \ell_2)^2 - m^2]^C}, \tag{6.2}$$

where $D = 5 - 2\epsilon$. We first look at the SL(2) subalgebra which excludes the trace part of the GL(2) generators. For example, the SL(2) generator,

$$\Omega_{ij} = \begin{pmatrix} 1 & 0 \\ 0 & -1 \end{pmatrix}, \tag{6.3}$$

produces the IBP relation

$$0 = \int \frac{d^D \ell_1}{(2\pi)^D} \frac{d^D \ell_2}{(2\pi)^D} \left(\ell_1^\mu \frac{\partial}{\partial \ell_1^\mu} - \ell_2^\mu \frac{\partial}{\partial \ell_2^\mu} \right) \frac{1}{(\ell_1^2 - m^2)^A (\ell_2^2 - m^2)^B [(\ell_1 - \ell_2)^2 - m^2]^C}$$
$$= (-2A + 2B) V_{A,B,C} - 2C V_{A-1,B,C+1} + 2C V_{A,B-1,C+1} + m^2 (-2A V_{A+1,B,C} + 2B V_{A,B+1,C}), \tag{6.4}$$

where we used $A + B + C = 5$. The second-to-last line of the above equation contains integrals that are logarithmically divergent in the ultraviolet, while the last line contains integrals that are ultraviolet finite by power counting—as indicated by simple considerations of dimensional analysis, since the last line is proportional to m^2. Absence of subdivergences implies that *overall* power counting is sufficient for showing whether an integral is ultraviolet finite. Therefore, for the purpose of extracting ultraviolet divergences, we can disregard the last line of the above equations, and instead work with an IBP system *modulo finite integrals*. Since the generators of the SL(2)

subalgebra are traceless, the IBP relations we generate have no explicit dependence on the dimension D.

Inspecting Eq. (6.4) we see that, setting $m = 0$ from the beginning removes the last line of that equation while preserving the relation between integrals exhibiting ultraviolet poles. Thus, even though setting $m = 0$ turns these vacuum integrals into scaleless integrals that vanish in dimensional regularization, the SL(2) subalgebra nonetheless generates the correct IBP relations between ultraviolet poles. In contrast, including the trace generator,
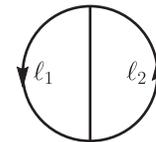
FIG. 19. Two-loop example for illustrating SL(L) symmetry.

---

[6]We have already performed expansion in the ultraviolet region to produce vacuum integrals, but even the (infrared-regulated) vacuum integrals contain finite parts that are not of interest to us here.

$$\Omega_{ij} = \begin{pmatrix} 1 & 0 \\ 0 & 1 \end{pmatrix}, \tag{6.5}$$

which extends SL(2) to GL(2), requires nonvanishing m. Indeed, this generator produces the IBP relations

$$\begin{aligned} 0 &= \int \frac{d^D \ell_1}{(2\pi)^D} \frac{d^D \ell_2}{(2\pi)^D} \frac{\partial}{\partial \ell_i^\mu} \frac{\ell_i^\mu}{[(\ell_1)^2 - m^2]^A [(\ell_2)^2 - m^2]^B [(\ell_1 - \ell_2)^2 - m^2]^C} \\ &= -4\epsilon V_{A,B,C} - 10m^2 (V_{A+1,B,C} + V_{A,B+1,C} + V_{A,B,C+1}). \end{aligned} \tag{6.6}$$

If we set $m = 0$, the above relations imply that $V_{A,B,C} = 0$. The factor (-4ϵ) is expected because the diagonal transformation probes the scaling weight of the integral, which would be exactly zero in $D = 5$. As long as the IBP relations corresponding to the trace part of GL(2) are omitted, the IBP system no longer sets to zero massless vacuum integrals and correctly reflects the ultraviolet poles of these integrals without contamination from IR poles.

The above argument straightforwardly carries over to the five-loop vacuum integrals in $D = 24/5 - 2\epsilon$, since no subdivergences exist in this dimension. The resulting IBP system only involves logarithmically divergent vacuum integrals, and does not include any finite integrals or power-divergent integrals (which do not produce poles in dimensional regularization). This enormously reduces the size of the linear system to be solved.

A useful property of the SL(L)-generated IBP system is that, even though each vacuum integral depends on the dimension D implicitly, the relations between them do not contain any explicit dependence on D [8]. This fact appears to help explain the observations in Sec. VII.

B. The IBP system at five loops

The complete set of integral topologies—suppressing dots or numerators—that we need to consider for the reduction of the vacuum integrals of the five-loop four-point $\mathcal{N} = 8$ supergravity amplitude is shown in Fig. 14. This list does not include any diagram that factorizes, such as those illustrated in Fig. 13. It also removes integrals related to kept ones by identities between integrals not isomorphic to each other, such as those illustrated in Fig. 17.

By acting with the SL(5) generators on all logarithmically divergent canonical integrals with up to four dots, we find IBP relations between vacuum integrals with up to five dots, the additional dot following from acting with derivatives on propagators. While such integrals do not appear in the expansion of the integrand in $D = 24/5$, they are necessary for finding the relations between integrals with four dots. We also include relations between integrals generated by graph automorphisms which transform nontrivially the numerator factors, as illustrated in Fig. 18. In these relations, all the integrals are mapped to canonical integrals using enhanced graph isomorphisms as described

in Sec. IV C. Because of their similarity with the IBP relations it is convenient to solve them simultaneously. The solution to this system of equations expresses all needed vacuum integrals in terms of master integrals.

As a warm up to setting up and solving the IBP system for the supergravity problem in $D = 24/5$, we solved the much simpler cases of $\mathcal{N} = 8$ supergravity in $D = 22/5$ and $\mathcal{N} = 4$ super-Yang-Mills theory in $D = 26/5$. The integrals which appear in both these simpler cases have at most two dots and thus, the IBP system contains integrals with up to three dots. In the case of $\mathcal{N} = 8$ supergravity in $D = 22/5$, the three-dot system has 44 428 different integrals, and about 1.7×10^5 linear relations generated. The simpler numerator factors of $\mathcal{N} = 4$ super-Yang-Mills make this case much simpler, containing only 5 975 distinct integrals and about 9 900 linear relations between them. The solution of the latter system expresses all the two-dot vacuum integrals, divergent in $D = 26/5$, in terms of the 16 master vacuum integrals displayed in Fig. 20.

For the main problem of $\mathcal{N} = 8$ supergravity in $D = 24/5$ with the improved integrand obtained in Sec. III, we have to reduce integrals with up to four dots. There are 141 592 distinct integrals of this type. The relevant five-dot system has 3 687 534 integrals of which 845 323 are distinct. The SL(5) transformations generate about 2.8×10^6 IBP relations, while numerator-changing isomorphisms generate about 9×10^5 further relations. This system is straightforward to solve using sparse Gaussian elimination and finite-field methods [79]; we used the linear system solver LinBox [80], and confirmed the solution with FinRed [81]. The result is that all vacuum integrals for the expansion of $\mathcal{N} = 8$ supergravity amplitude in $D = 24/5$ are expressed as linear combinations of the eight master integrals shown in Fig. 21.

C. Result for ultraviolet divergences

As a first test for the full calculation, we used the reduction of the vacuum integrals to verify that our integrand exhibits the known ultraviolet properties in $D = 22/5$. We find that, as expected, all vacuum integrals cancel after IBP reduction, the five-loop four-point $\mathcal{N} = 8$ amplitude is ultraviolet finite,
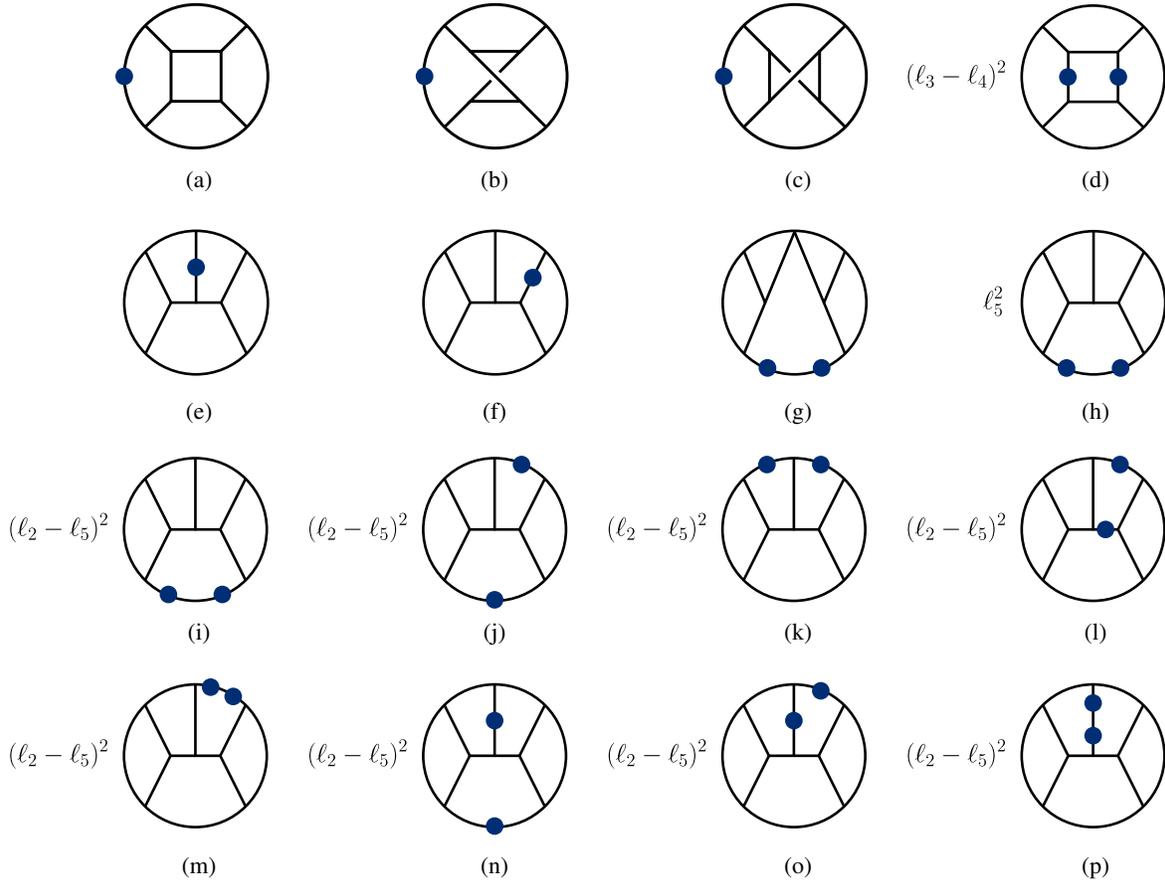
FIG. 20. The sixteen master integrals to which any five-loop vacuum integrals in $\mathcal{N} = 4$ super-Yang-Mills with up to two dots can be reduced. The dots represent repeated propagators. The labels of the diagrams match those of Fig. 15. We shall refer to the corresponding integrals either through their graph or as $I_{(a)}$, $I_{(b)}$, etc.

$$\mathcal{M}_4^{(5)}|_{\text{leading}}^{D=22/5} = 0. \tag{6.7}$$

With our new integrand there are few potential contributions because the naive double-copy terms are manifestly ultraviolet finite in $D = 22/5$ and only the contact terms give potential contributions. A similar check is performed for the earlier form of the integrand in Ref. [28], but that case only confirms the cancellation of the vacuum diagrams with the maximum imposed.

As another test of our approach, we also recovered the leading divergence of $\mathcal{N} = 4$ super-Yang-Mills theory in its five-loop critical dimension, $D = 26/5$, originally found in [32]. Starting from our improved $\mathcal{N} = 4$ super-Yang-Mills integrand of Sec. III, extracting the leading divergence in terms of vacuum integrals and then substituting their expressions in terms of master integrals, we obtain

$$\mathcal{A}_4^{(5)}\Big|_{\text{leading}} = \frac{144}{5} g^{12} st A^{\text{tree}} N_c^3 \left(N_c^2 \,\raisebox{-1em}{\includegraphics{}} + 48 \left(\frac{1}{4} \,\raisebox{-1em}{\includegraphics{}} + \frac{1}{2} \,\raisebox{-1em}{\includegraphics{}} + \frac{1}{4} \,\raisebox{-1em}{\includegraphics{}} \right) \right)$$
$$\times \left(t\, \tilde{f}^{a_1 a_2 b} \tilde{f}^{b a_3 a_4} + s\, \tilde{f}^{a_2 a_3 b} \tilde{f}^{b a_4 a_1} \right). \tag{6.8}$$

The $\tilde{f}^{abc}$ are the group structure constants, as normalized below Eq. (2.1), and the s and t are the usual Mandelstam invariants. Here $A^{\text{tree}} \equiv A^{\text{tree}}(1, 2, 3, 4)$ is the color-ordered tree amplitude with the indicated ordering of external legs. This reproduces the result of Ref. [32], providing a nontrivial check of both our gauge-theory integrand construction and IBP reductions methods.
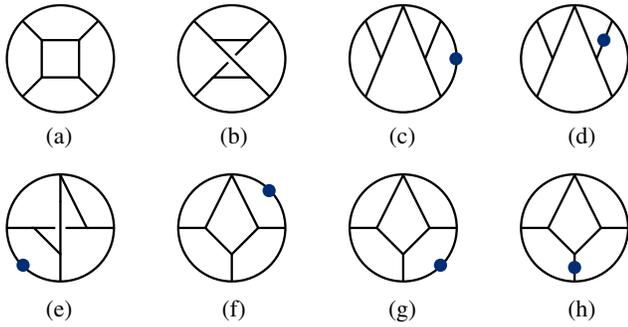
FIG. 21. The eight master integrals to which any five-loop vacuum integrals in $\mathcal{N} = 8$ supergravity with up to four dots can be reduced. The dots represent repeated propagators. We shall refer to the corresponding integrals either through their graph or as $I_{(a)}$, $I_{(b)}$, etc.

Interestingly, the thirteen master integrals in Fig. 20 that have vanishing coefficients in Eq. (6.8) violate a "no-one-loop-triangle" rule.[7] Indeed, diagrams (e)–(p) contain one-loop triangle subdiagrams while diagram (d) contains a loop momentum-dependent numerator in one-loop box subdiagrams, which upon expanding and reducing of that one-loop subintegral also leads to triangle subintegrals. Another interesting feature of these results is that the relative factors of the subleading-color term are given by the symmetry factors of the corresponding integrals. In the next section, we will show that these observations are part of a more general pattern.

Extracting the leading ultraviolet terms for $\mathcal{N} = 8$ supergravity in $D = 24/5$ follows the same strategy. After reducing the vacuum integrals obtained from our improved integrand to the basis of master integrals we find

$$\mathcal{M}_4^{(5)}\Big|_{\text{leading}} = -\frac{16 \times 629}{25}\left(\frac{\kappa}{2}\right)^{12}(s^2 + t^2 + u^2)^2 stu M_4^{\text{tree}}\left(\frac{1}{48}\,\includegraphics{box} + \frac{1}{16}\,\includegraphics{cross}\right). \tag{6.9}$$

This is the same result as obtained in the previous section by assuming that only vacuum diagrams with maximal cuts contribute, and proves that Eq. (5.7) is complete. As in the case of the reduction of the expansion of the four-point five-loop $\mathcal{N} = 4$ super-Yang-Mills amplitude, all master integrals containing triangle subdiagrams, or with numerators which upon further one-loop reduction lead to triangle subdiagrams, enter with vanishing coefficients. Moreover, similarly to the subleading color in the gauge-theory case, the relative coefficients between the integrals are the symmetry factors of the vacuum diagrams. As we discuss in the next section, these observations do not appear to be accidental.

The two Wick-rotated vacuum integrals in Eq. (6.9) are both positive definite, proving that no further hidden cancellations are present. We evaluated numerically, using FIESTA [82], the two master integrals entering Eq. (6.9), given by diagrams (a) and (b) in Fig. 21, and find

$$V_5^{(a)} = \frac{1}{(4\pi)^{12}}\frac{0.563}{\epsilon}, \qquad V_5^{(b)} = \frac{1}{(4\pi)^{12}}\frac{0.523}{\epsilon}. \tag{6.10}$$

The dimensional-regularization parameter is $\epsilon = (24/5 - D)/2$. Using Eq. (6.9), the numerical value of the divergence is

$$\mathcal{M}_4^{(5)}\Big|_{\text{leading}} = -17.9\left(\frac{\kappa}{2}\right)^{12}\frac{1}{(4\pi)^{12}}(s^2 + t^2 + u^2)^2 stu M_4^{\text{tree}}\frac{1}{\epsilon}. \tag{6.11}$$

We leave as a problem for the future the question of obtaining an exact analytic expression instead of the numerical one found here.

VII. OBSERVATIONS ON ULTRAVIOLET CONSISTENCY

Given the wealth of results from previous papers [13,18–21,32,83], as well as those from Sec. VI, we are in the position to search for useful structures that can lead to a more economic identification of the leading ultraviolet behavior of $\mathcal{N} = 4$ super-Yang-Mills theory and $\mathcal{N} = 8$ supergravity. In this section we analyze the available results in both these theories, observing remarkable consistency and recursive properties, whereby leading L-loop ultraviolet divergences in the L-loop critical dimension appear to be tightly constrained by the lower-loop vacuum diagrams describing leading behavior in the lower-loop critical dimension.

First we collect the known results for the leading ultraviolet behavior of both $\mathcal{N} = 4$ super-Yang-Mills theory and $\mathcal{N} = 8$ supergravity. We then demonstrate that appropriately defined subdiagrams of the vacuum diagrams are simply related to the vacuum diagrams describing lower-loop leading ultraviolet behavior.

---

[7]When counting the number of propagators around a loop, each dot should be counted as well.

Within the generalized-unitarity method, higher-loop scattering amplitudes are constructed in terms of lower-loop ones. The one-particle cut, setting on shell a single propagator, provides a direct link between L-loop n-point amplitudes and $(L-1)$-loop $(n+2)$-point amplitudes. One may therefore suspect that there may exist a relation between the leading ultraviolet properties of these amplitudes in their respective critical dimensions, which echoes the relation between the complete amplitudes. We will find, however, more surprising consistency relations between the leading ultraviolet behavior of L- and $(L-1)$-loop amplitudes with the same number of external legs for $L \leq 6$ for $\mathcal{N} = 4$ super-Yang-Mills theory and for $L \leq 5$ for $\mathcal{N} = 8$ supergravity. The nontrivial manipulations necessary for extracting the leading ultraviolet divergence adds to the surprising features of these relations. Indeed, without appropriate choices of integral bases, they would be obfuscated. They point to the possibility of a principle governing perturbative consistency in the ultraviolet. We close by noting the possibility that one may exploit these patterns to directly make detailed predictions of ultraviolet properties at higher-loop orders.

A. Review of results

After IBP reduction, we obtain a simple description of the leading ultraviolet behavior in terms of a set of master vacuum integrals defined as

TABLE II. The critical dimensions where ultraviolet divergences first occur in $\mathcal{N} = 4$ super Yang-Mills theory and $\mathcal{N} = 8$ supergravity, as determined by explicit calculations.

Loops	D_c for $\mathcal{N} = 4$ sYM	D_c for $\mathcal{N} = 8$ Supergravity
1	8	8
2	7	7
3	6	6
4	11/2	11/2
5	26/5	24/5
6	5	$\cdots$

$$V = -i^{L+\sum_j A_j} \int \prod_{i=1}^{L} \frac{d^D \ell_i}{(2\pi)^D} \prod_j \frac{1}{(p_j^2 - m^2)^{A_j}}, \quad (7.1)$$

where the p_i are linear combinations of the independent loop momenta and the A_i are the propagators' exponents. The number of dots on propagator j is $A_j - 1$ for $A_j \geq 2$ The indices can be negative, in which case they represent irreducible numerators, as discussed in Sec. VI. While there is no need to explicitly introduce a mass regulator for carrying out the IBP reductions, we do so here to make the integrals well defined in the infrared.

Collecting the results from Refs. [13,18–20] and from Eq. (6.9), the leading ultraviolet behavior of $\mathcal{N} = 8$ supergravity at each loop order through five loops is described by vacuum diagrams as

$$(7.2)$$

where the universal factor is $\mathcal{K}_G \equiv stu M_4^{\text{tree}}(1, 2, 3, 4)$. For each loop order, the critical dimension is different and is summarized in Table II.

We also collect all known vacuum graph expressions of the leading ultraviolet behavior in the maximally supersymmetric $SU(N_c)$ Yang-Mills theory [13,18,20,21,32,83],

$$\mathcal{A}_4^{(1)}\Big|_{\text{leading}} = g^4 \mathcal{K}_{\text{YM}} \left(N_c(\tilde{f}^{a_1 a_2 b}\tilde{f}^{b a_3 a_4} + \tilde{f}^{a_2 a_3 b}\tilde{f}^{b a_4 a_1}) - 3 B^{a_1 a_2 a_3 a_4}\right)\; \bigcirc,$$

$$\mathcal{A}_4^{(2)}\Big|_{\text{leading}} = - g^6 \mathcal{K}_{\text{YM}} \left[F^{a_1 a_2 a_3 a_4}\left(N_c^2\; \bigcirc + 48\left(\frac{1}{4}\; \bigcirc + \frac{1}{4}\; \bigcirc\right)\right)\right.$$

$$\left. + 48\, N_c\, G^{a_1 a_2 a_3 a_4}\left(\frac{1}{4}\; \bigcirc + \frac{1}{4}\; \bigcirc\right)\right],$$

$$\mathcal{A}_4^{(3)}\Big|_{\text{leading}} = 2\, g^8\, \mathcal{K}_{\text{YM}}\, N_c F^{a_1 a_2 a_3 a_4}\left(N_c^2\; \bigcirc + 72\left(\frac{1}{6}\; \bigcirc + \frac{1}{2}\; \bigcirc\right)\right),$$

$$\mathcal{A}_4^{(4)}\Big|_{\text{leading}} = -6\, g^{10}\, \mathcal{K}_{\text{YM}}\, N_c^2 F^{a_1 a_2 a_3 a_4}\left(N_c^2\; \triangle + 48\left(\frac{1}{4}\; \triangle + \frac{1}{2}\; \triangle + \frac{1}{4}\; \triangle\right)\right),$$

$$\mathcal{A}_4^{(5)}\Big|_{\text{leading}} = \frac{144}{5} g^{12}\mathcal{K}_{\text{YM}}\, N_c^3\, F^{a_1 a_2 a_3 a_4}\left(N_c^2\; \square + 48\left(\frac{1}{4}\; \square + \frac{1}{2}\; \boxtimes + \frac{1}{4}\; \boxtimes\right)\right),$$

$$A_4^{(6)}\Big|_{\text{leading}} = -120 g^{14}\mathcal{K}_{\text{YM}}\, F^{a_1 a_2 a_3 a_4} N_c^6 \left(\frac{1}{2}\; \pentagon + \frac{1}{4}(\ell_1 + \ell_2)^2\; \pentagon_{1}^{2} - \frac{1}{20}\; \pentagon\right)$$

$$+ \mathcal{O}(N_c^4),$$

$$(7.3)$$

where the universal factor is $\mathcal{K}_{\text{YM}} \equiv st A_4^{\text{tree}}(1, 2, 3, 4)$, and

$$F^{a_1 a_2 a_3 a_4} \equiv t\tilde{f}^{a_1 a_2 b}\tilde{f}^{b a_3 a_4} + s\tilde{f}^{a_2 a_3 b}\tilde{f}^{b a_4 a_1},$$

$$G^{a_1 a_2 a_3 a_4} \equiv s\delta^{a_1 a_2}\delta^{a_3 a_4} + t\delta^{a_4 a_1}\delta^{a_2 a_3} + u\delta^{a_1 a_3}\delta^{a_2 a_4},$$

$$B^{a_1 a_2 a_3 a_4} \equiv \tilde{f}^{a_1 b_1 b_2}\tilde{f}^{a_2 b_2 b_3}\tilde{f}^{a_3 b_3 b_4}\tilde{f}^{a_4 b_4 b_1}. \qquad (7.4)$$

As before, $\tilde{f}^{abc}$ are the group structure constants, with normalization given below Eq. (2.1). As in the gravity case, the critical dimension at each loop order is different, and is included in Table II.

Inspecting Eqs. (7.2) and (7.3) we already note a remarkable property in both the supergravity and subleading-color gauge-theory expressions: the relative coefficients between vacuum integrals in these representations, ignoring signs, are given by the symmetry factors of the corresponding vacuum graphs. For example, at five loops in Eq. (7.2), the first vacuum graph has 48 automorphisms and the second has 16 automorphisms, matching the relative factors. While the amplitude has such coefficients for each integral [see e.g., Eq. (3.3)], their appearance in the leading ultraviolet divergence is unexpected due to both the nontrivial manipulations and the choices of master integrals that are required to arrive at the final result.

Further inspection of Eqs. (7.2) and (7.3) reveals further interesting structures, showing that the relative coefficients of vacuum integrals are consistently related between the different loop orders.

B. Observed ultraviolet consistency

An L-loop (vacuum) integral has many $L' < L$ subintegrals. A way to isolate one and expose its associated ultraviolet properties is to take its loop momenta to be much larger than the other $(L - L')$ ones. We define an L'-loop subdiagram of an L-loop diagram as the sum over all of its L'-loop subintegrals. Since each subintegral may have a different critical dimension, the critical dimension of an L'-loop subdiagram is the minimum of the critical dimensions of all the L'-loop subintegrals.

With this definition, to compare the higher- and lower-loop leading ultraviolet properties of four-point amplitudes we carry out the following steps:
  (1) For each L-loop vacuum diagram construct its L'-loop subdiagram.
  (2) Keep only those contributions with leading ultraviolet behavior, i.e., those that are divergent in the lowest critical dimension.

(3) Apply IBP identities, as needed, to map the lower-loop vacuum integrals into the same vacuum integral basis as the one used in the ultraviolet expansion of the lower-loop amplitude.

As we now show by example, every result in Eqs. (7.2) and (7.3) supports the observation that the leading ultraviolet behavior at L and L' loops in their respective critical dimensions are consistent.

To see the power of this observation, consider the all-order constraints from one-loop subdiagrams. From Eqs. (7.2) and (7.3), we see that the one-loop leading ultraviolet divergence is given by a vacuum integral with four propagators. For the higher-loop vacuum graphs this amounts to the statement that there exists an integral basis such that all one-loop subloops of any higher -loop vacuum must contain at least four propagators.[8] This is equivalent to the no-triangle property of one-loop amplitudes in both $\mathcal{N} = 8$ and $\mathcal{N} = 4$ super-Yang-Mills amplitudes [84], except that here it applies to the reduction to an integral basis of the vacuum integrals describing the leading ultraviolet behavior. One-loop subgraphs with more than four propagators give a subleading behavior which we discard according to our procedure which focuses on the leading ultraviolet properties. Because there is only a single type of leading one-loop subdiagram, this property of one-loop subgraphs places no constraint on the relative coefficients of the higher-loop vacuum graphs. Nevertheless, the constraint that each one-loop subgraph has at least four propagators is extremely powerful. In particular, as discussed in Sec. VI, the only integrals in our basis of five-loop vacuum integrals without triangle subdiagrams are the two five-loop integrals contributing to Eq. (7.2). A similar property holds for $\mathcal{N} = 4$ super-Yang-Mills theory, where the only five-loop vacuum integral basis elements without any triangle or bubble subintegrals are the ones appearing in Eq. (7.3). This is quite a remarkable property because, in an appropriately chosen integral basis that maximizes the number of one-loop triangle and bubble subintegrals, it severely limits the vacuum integrals that can appear in the final expressions.

While the one-loop properties discussed above should hold for each one-loop subintegral at any loop order, understanding the consequences of higher-loop ultraviolet divergences in (7.2) and (7.3) can be best appreciated via a case by case analysis. We choose three illustrative examples. We begin by showing the consistency of subleading-color $\mathcal{N} = 4$ super-Yang-Mills between five and four loops. We focus on the subleading-color part, because it has a more complex structure than the leading-color part

---

[8] In an arbitrary integral basis this property is not manifest and emerges only after the summation over all one-loop subintegrals of all diagrams and reduction to a one-loop integral basis.

and it is similar to the supergravity case. We then examine the consistency of the four-loop ultraviolet divergences with those at lower loops, which are the same for the $\mathcal{N} = 4$ super-Yang-Mills theory at subleading color and the $\mathcal{N} = 8$ supergravity. Last, we discuss the five-to-four loop consistency of our results for the five-loop $\mathcal{N} = 8$ supergravity.

As mentioned earlier, not all terms in the sum that defines a lower-loop subdiagram have the same critical dimension. For example, when relating L and $(L - 1)$-loop diagrams, excluding a dotted propagator leads to a term with a lower critical dimension than one obtained by excluding an undotted one. Thus, when focusing on the ultraviolet critical dimension of lower-loop diagrams it suffices to keep only terms obtained by disconnecting the propagators with the largest number of dots. Once the subdiagrams are identified, we can compare them to the lower-loop result by treating the subdiagram as a new vacuum diagram where we have kept the leading order in small-momentum expansion for the excluded leg. This results in lower-loop vacuum diagrams with dots on the propagators where the excluded leg is connected to the subgraph.

For the $\mathcal{N} = 4$ super-Yang-Mills five-loop vacuum diagrams, the leading four-loop subdiagrams are all those that exclude the leg that carries the dot. Diagrammatically, we write

$$(7.5)$$

Excluding the propagator outside the dashed box and taking its momentum small compared to the remaining ones leads to

$$(7.6)$$

This exactly matches the subleading-color four-loop vacuum diagrams describing their relative coefficients in Eq. (7.3).

Showing the consistency of the four loop expression with lower loops follows similar steps. Now there are two dotted legs that can be excluded. Summing over the two expansions of each subdiagram, we find

$$\text{(diagrams)} \to 2 \text{(diagram)}, \qquad \text{(diagrams)} \to 2 \text{(diagram)}, \qquad \text{(diagrams)} \to 2 \text{(diagram)}. \tag{7.7}$$

Using this we see that the subdiagrams match the relative factors and three-loop vacuum diagrams in Eq. (7.3),

$$\text{(diagram)} \to 3 \left(\frac{1}{6} \text{(diagram)} + \frac{1}{2} \text{(diagram)} \right). \tag{7.8}$$

Additionally, we can extract the two-loop subdiagrams in the four-loop divergence by expanding around both dotted propagators. This gives

$$\text{(diagram)} \to \text{(diagram)}, \qquad \text{(diagram)} \to \text{(diagram)}, \qquad \text{(diagram)} \to \text{(diagram)}. \tag{7.9}$$

Using this we find that with the relative coefficients from the four-loop expression, these subdiagrams are also consistent with the leading lower-loop behavior

$$\text{(diagram)} \to \frac{1}{4} \text{(diagram)} + \frac{1}{4} \text{(diagram)}. \tag{7.10}$$

It is straightforward to confirm that the same relative coefficients arise by starting from the three-loop expression in Eq. (7.8) and extracting the leading two-loop subdiagrams.

Since master integrals giving the ultraviolet divergence of the five-loop supergravity amplitude in $D = 24/5$ do not have doubled propagators, all ways of excluding one propagator lead to integrals of the same critical dimension and must therefore be kept. The planar diagram is a cube, so all of its edges are equivalent. Summing over all the four-loop subintegrals leads to

$$\text{(diagram)} \to 12 \text{(diagram)}. \tag{7.11}$$

The nonplanar diagram has two inequivalent types of legs to exclude. There are eight legs that, when expanded around, lead to a planar four-loop subdiagram. The other four legs lead to a nonplanar subdiagram. Thus, after isomorphisms, the subintegrals of the nonplanar five-loop diagram contribute

$$\text{(diagram)} \to 8 \text{(diagram)} + 4 \text{(diagram)}. \tag{7.12}$$

After accounting for the relative symmetry factors of $1/48$ and $1/16$ between the two five-loop diagrams in Eq. (7.2), we get

$$\text{(diagram)} \to \frac{1}{4} \text{(diagram)} + \frac{1}{2} \text{(diagram)} + \frac{1}{4} \text{(diagram)}, \tag{7.13}$$

matching the relative factors between the four-loop vacuum diagrams also given in Eq. (7.2).

Through four loops super-Yang-Mills subleading-color and supergravity divergences follow the same pattern, being related between different loop orders by removing a dotted propagator. While in both theories the consistency relations hold at five loops as well, they now involve removing a dotted and an undotted propagator, respectively. The additional propagator in the gauge-theory expression raises its critical dimension to $D = 26/5$. It is remarkable that, even though the various integrals and symmetry factors at five loops differ in the two theories, consistency requires that the relative coefficients for four-loop subdiagrams are the same.

Let us elaborate briefly on the structure of the planar $\mathcal{N} = 4$ super-Yang-Mills vacuum integrals at six loops. Unlike the previous examples, the lower-loop integrals given by our construction are not among the five-loop master integrals in Fig. 20 and a comparison with the five-loop expression (7.3) requires use of IBP identities. As in the five-to-four loop relation, the integrals with lowest critical dimension arise from subdiagrams that exclude the doubled propagator in the six-loop vacuum diagrams. Thus, the leading five-loop subdiagram result is

$$\text{(image)} \rightarrow \frac{1}{2} \text{(image)} + \frac{1}{4}(\ell_1 + \ell_2)^2 \text{(image)} + \text{subleading color}. \tag{7.14}$$

Using an integration-by-parts relation [see Eq. (4) of Ref. [32]]

$$\frac{1}{2} \text{(image)} + \frac{1}{4}(\ell_1 + \ell_2)^2 \text{(image)} = \frac{6}{5} \text{(image)}, \tag{7.15}$$

to map (7.14) to the five-loop integral basis, we find that it is proportional to the five-loop leading color term in Eq. (7.3). It is gratifying that the subdiagram consistency holds even if not initially obvious.

C. Applications

The consistency observations discussed above give us additional confidence that we have correctly computed the leading ultraviolet behavior of $\mathcal{N} = 8$ supergravity at five loops by showing that in the sense discussed above, it fits the pattern of ultraviolet properties at all lower loops. The simple structures at the vacuum diagram level uncovered here also offer the exciting possibility of probing seemingly out of reach ultraviolet properties at even higher loops. Apart from the possibility of imposing them on an ansatz for the leading ultraviolet terms of gauge and gravity amplitudes, we can use them to simplify the IBP system by focusing only on the vacuum integrals that are expected to appear. For example, in Sec. V we vastly simplified the five-loop $\mathcal{N} = 8$ IBP system by assuming that only the vacuum integrals with maximal cuts survive in the final result. As emphasized above, this condition follows from demanding consistency of the five-loop vacuum master diagrams with one-loop subdiagrams, which rules out one-loop triangle subgraphs and all but two five-loop master vacuum diagrams in the basis of Fig. 21. More importantly this condition eliminates nearly all integrals from the IBP system as well as a substantial part of the expansion of the integrand. The same strategy should continue to be fruitful at even higher-loop orders. Alternatively, it may be possible to completely bypass the construction of the integrand, its ultraviolet expansion and integration, and instead extrapolate the final result in terms of vacuum diagrams to higher-loop orders. We leave this task for future study.

We emphasize that the observed ultraviolet consistency is a property of the leading behavior after simplifying the integrals via Lorentz invariance and integration-by-parts relations. It relies on nontrivial simplifications that occur in the integral reduction and is manifest because we judiciously chose the vacuum integral bases. A key property of

our IBP systems is that the space-time dimension enters only implicitly through the critical dimension where the integrals are logarithmically divergent. Had there been explicit dependence on the dimension, one would naturally expect a nontrivial dependence on dimension in the relative coefficients of master integrals and thus, given the differing critical dimensions at different loop orders, it would disrupt any systematic cross-loop-order relations. Simplifications based on Lorentz invariance in Eqs. (4.5) and (4.6) were used, and introduce explicit dependence on dimension. It is rather striking that this dependence drops out once the IBP relations are used and consequently it does not complicate relations between vacuum diagrams and their subdiagrams. These properties are worth investigating.

VIII. CONCLUSIONS AND OUTLOOK

In this paper we determined the ultraviolet behavior of the five-loop four-point amplitude of $\mathcal{N} = 8$ supergravity, finding the critical dimension where it first diverges to be $D_c = 24/5$. In analyzing the results we made the rather striking observation that the vacuum diagrams that describe the leading ultraviolet behavior satisfy certain nontrivial relations to the analogous lower-loop vacuum diagrams.

Previous work found examples of enhanced ultraviolet cancellations that render ultraviolet finite [5,6] certain amplitudes in $\mathcal{N} = 4$ and $\mathcal{N} = 5$ supergravity in $D = 4$, despite the possibility of counterterms allowed by all known symmetry considerations [9,17]. Related arguments suggest that $\mathcal{N} = 8$ supergravity should diverge at five loops in $D = 24/5$ [16]. While one might have suspected that there could be corresponding enhanced cancellations in $\mathcal{N} = 8$ supergravity at five loops, our results conclusively demonstrate that, at this loop order, there are no further cancellations of ultraviolet divergences beyond those identified by symmetry arguments.

The divergence we find in $D = 24/5$ at five loops corresponds to a $D^8 R^4$ counterterm. This counterterm is especially interesting because it corresponds to a potential $D = 4$ divergence believed to be consistent with the $E_{7(7)}$ duality symmetry of maximal supergravity. It is, however, not clear that our result in $D = 24/5$ points towards a seven-loop divergence in $D = 4$, because the existence of counterterms does not transfer trivially between dimensions and loop orders. For example, one might be tempted to argue for a three-loop divergence in $\mathcal{N} = 4$ or $\mathcal{N} = 5$ supergravity in $D = 4$ based on the existence [7] of a nonvanishing one-loop R^4 counterterm in $D = 8$ in both theories; we know however that both theories are finite at

three loops [5,6]. Another result that indicates that further investigation of the ultraviolet structure of supergravities in four dimensions is warranted is the suspected link between anomalies and divergences in supergravity theories on the one hand, and the anticipated lack of anomalies in theories with $\mathcal{N} \geq 5$ supersymmetry on the other [10,11]. Of course, not every divergence necessarily has an anomaly behind it. Nevertheless, it is surprising that $\mathcal{N} = 5$ supergravity at four loops in $D = 4$ appears to have additional cancellations beyond those predicted by symmetry considerations [6], while $\mathcal{N} = 8$ supergravity at five loops in $D = 24/5$ does not.

The ultraviolet properties of the amplitude were extracted, following standard methods [69], by expanding the integrand at large loop momenta or equivalently small external momenta, to identify the logarithmic divergences in various dimensions. The result was then reduced to a combination of master integrals; to this end we made use of modern ideas of organizing the system of IBP identities in terms of an SL(L) symmetry [8] (where L is the number of loops) and restricting to integrals with leading ultraviolet behavior. In addition to integrating the complete expansion of a new integrand in both $D = 22/5$ and $D = 24/5$, we also integrated the expansion of the previously obtained integrand [28] in these dimensions, under the assumption that the only master integrals that appear in the final result have maximal cuts. These results, obtained by using unitarity-compatible integration-by-parts techniques [37,39], agree with those of the full integration of the simpler integrand, thus providing a highly nontrivial check of our calculations.

The agreement of the two approaches highlights an important trend: the only integrals that contribute to the divergence of the four-point $1 \leq L \leq 5$ amplitudes in their critical dimensions are those with maximal cuts at the vacuum level. At higher loops we expect a systematic application of similar considerations to lead to a drastic reduction in the computational complexity. An approach based on exploiting these observations may make it possible to directly determine the critical dimension of the six- and seven-loop $\mathcal{N} = 8$ supergravity amplitudes.

An even greater efficiency gain may lie in the observed ultraviolet consistency relations described in Sec. VII. That is, L'-loop subdiagrams of the leading ultraviolet divergence in the L-loop critical dimension reproduce, upon reduction to master integrals, the combination of vacuum diagrams describing the leading ultraviolet behavior in the L'-loop critical dimension. Moreover, in an appropriate basis, the relative coefficients of the vacuum master integrals are given by the order of the automorphism groups of the diagrams. We also observed similar patterns

in the vacuum diagrams of $\mathcal{N} = 4$ super-Yang-Mills theory through six loops, suggesting that they will continue to hold to higher-loop orders in both theories. While these observations are likely connected to standard consistency relations between multiloop amplitudes and their subamplitudes, in our case they remain a conjecture due to the nontrivial steps needed to relate an amplitude to a basis of master vacuum graphs in the critical dimension. These vacuum diagram patterns should be very helpful to identify those terms in higher-loop amplitudes that are important for determining the leading ultraviolet behavior, and for enormously simplifying the integration-by-parts system. By enforcing the patterns described here, it may even be possible to obtain detailed higher-loop information including a determination of the critical dimensions, bypassing the construction of complete loop integrands.

In summary, the success of the newly developed generalized double-copy construction [27,28], and integration tools [8,37–39,79–81] used in our five-loop calculations, as well as our observed vacuum subdiagram consistency constraints, indicates that problems as challenging as seven-loop $\mathcal{N} = 8$ supergravity in four dimensions may now be within reach of direct investigations.

[1] D. Z. Freedman, P. van Nieuwenhuizen, and S. Ferrara, Progress toward a theory of supergravity, Phys. Rev. D **13**, 3214 (1976); S. Deser and B. Zumino, Consistent supergravity, Phys. Lett. **62B**, 335 (1976).

[2] Z. Bern, L. J. Dixon, and R. Roiban, Is $N = 8$ supergravity ultraviolet finite?, Phys. Lett. B **644**, 265 (2007); Z. Bern, J. J. Carrasco, D. Forde, H. Ita, and H. Johansson, Unexpected cancellations in gravity theories, Phys. Rev. D **77**, 025010 (2008); E. Herrmann and J. Trnka, Gravity on-shell diagrams, J. High Energy Phys. 11 (2016) 136.

[3] E. Cremmer, J. Scherk, and S. Ferrara, SU(4) invariant supergravity theory, Phys. Lett. **74B**, 61 (1978); A. K. Das, SO(4) invariant extended supergravity, Phys. Rev. D **15**, 2805 (1977); E. Cremmer and J. Scherk, Algebraic simplifications in supergravity theories, Nucl. Phys. **B127**, 259 (1977).

[4] B. de Wit and H. Nicolai, Extended supergravity with local SO(5) invariance, Nucl. Phys. **B188**, 98 (1981).

[5] Z. Bern, S. Davies, T. Dennen, and Y.-t. Huang, Absence of Three-Loop Four-Point Divergences in $N = 4$ Supergravity, Phys. Rev. Lett. **108**, 201301 (2012).

[6] Z. Bern, S. Davies, and T. Dennen, Enhanced ultraviolet cancellations in $\mathcal{N} = 5$ supergravity at four loops, Phys. Rev. D **90**, 105011 (2014).

[7] Z. Bern, S. Davies, T. Dennen, and Y.-t. Huang, Ultraviolet cancellations in half-maximal supergravity, Phys. Rev. D **86**, 105014 (2012).

[8] Z. Bern, M. Enciso, J. Parra-Martinez, and M. Zeng, Manifesting enhanced cancellations in supergravity: integrands versus integrals, J. High Energy Phys. 05 (2017) 137.

[9] G. Bossard, P. S. Howe, and K. S. Stelle, Anomalies and divergences in $N = 4$ supergravity, Phys. Lett. B **719**, 424 (2013); Invariants and divergences in half-maximal supergravity theories, J. High Energy Phys. 07 (2013) 117; Z. Bern, S. Davies, and T. Dennen, Ultraviolet structure of half-maximal supergravity with matter multiplets at two and three loops, Phys. Rev. D **88**, 065007 (2013).

[10] N. Marcus, Composite anomalies in supergravity, Phys. Lett. **157B**, 383 (1985); J. J. M. Carrasco, R. Kallosh, R. Roiban, and A. A. Tseytlin, On the U(1) duality anomaly and the S-matrix of $N = 4$ supergravity, J. High Energy Phys. 07 (2013) 029; R. Kallosh, Cancellation of conformal and chiral anomalies in $\mathcal{N} \geq 5$ supergravities, Phys. Rev. D **95**, 041701 (2017); D. Z. Freedman, R. Kallosh, D. Murli, A. Van Proeyen, and Y. Yamada, Absence of U(1) anomalous superamplitudes in $\mathcal{N} \geq 5$ supergravities, J. High Energy Phys. 05 (2017) 067; Z. Bern, A. Edison, D. Kosower, and J. Parra-Martinez, Curvature-squared multiplets, evanescent effects, and the U(1) anomaly in $N = 4$ supergravity, Phys. Rev. D **96**, 066004 (2017); Z. Bern, J. Parra-Martinez, and R. Roiban, Cancelling the U(1) anomaly in the S-matrix of $N = 4$ supergravity, arXiv:1712.03928.

[11] Z. Bern, S. Davies, T. Dennen, A. V. Smirnov, and V. A. Smirnov, Ultraviolet Properties of $N = 4$ Supergravity at Four Loops, Phys. Rev. Lett. **111**, 231302 (2013).

[12] E. Cremmer, B. Julia, and J. Scherk, Supergravity theory in eleven dimensions, Phys. Lett. B **76**, 409 (1978); E. Cremmer and B. Julia, The $N = 8$ supergravity theory.

1. The Lagrangian, Phys. Lett. **80B**, 48 (1978); The SO(8) supergravity, Nucl. Phys. **B159**, 141 (1979).

[13] M. B. Green, J. H. Schwarz, and L. Brink, $N = 4$ Yang-Mills and $N = 8$ supergravity as limits of string theories, Nucl. Phys. **B198**, 474 (1982).

[14] P. S. Howe and U. Lindstrom, Higher order invariants in extended supergravity, Nucl. Phys. **B181**, 487 (1981); R. E. Kallosh, Counterterms in extended supergravities, Phys. Lett. **99B**, 122 (1981); M. T. Grisaru and W. Siegel, Supergraphity. 2. Manifestly covariant rules and higher loop finiteness, Nucl. Phys. **B201**, 292 (1982); Erratum: Supergraphity. 2. Manifestly covariant rules and higher loop finiteness, Nucl. Phys. **B206**, 496 (1982); N. Marcus and A. Sagnotti, The ultraviolet behavior of $N = 4$ Yang-Mills and the power counting of extended superspace, Nucl. Phys. **B256**, 77 (1985); G. Chalmers, On the finiteness of $N = 8$ quantum supergravity, arXiv:hep-th/0008162; N. Berkovits, New Higher-Derivative R^4 Theorems, Phys. Rev. Lett. **98**, 211601 (2007); M. B. Green, J. G. Russo, and P. Vanhove, Non-renormalization conditions in type II string theory and maximal supergravity, J. High Energy Phys. 02 (2007) 099; M. B. Green, J. G. Russo, and P. Vanhove, Ultraviolet Properties of Maximal supergravity, Phys. Rev. Lett. **98**, 131602 (2007); G. Bossard, P. S. Howe, and K. S. Stelle, The ultra-violet question in maximally supersymmetric field theories, Gen. Relativ. Gravit. **41**, 919 (2009); R. Kallosh, $N = 8$ supergravity on the light cone, Phys. Rev. D **80**, 105022 (2009); N. Berkovits, M. B. Green, J. G. Russo, and P. Vanhove, Non-renormalization conditions for four-gluon scattering in supersymmetric string and field theory, J. High Energy Phys. 11 (2009) 063.

[15] M. B. Green, J. G. Russo, and P. Vanhove, String-theory dualities and supergravity divergences, J. High Energy Phys. 06 (2010) 075; G. Bossard, P. S. Howe, and K. S. Stelle, On duality symmetries of supergravity invariants, J. High Energy Phys. 01 (2011) 020; N. Beisert, H. Elvang, D. Z. Freedman, M. Kiermaier, A. Morales, and S. Stieberger, E7(7) constraints on counterterms in $N = 8$ supergravity, Phys. Lett. B **694**, 265 (2010); P. Vanhove, The critical ultraviolet behavior of $N = 8$ supergravity amplitudes, arXiv:1004.1392.

[16] J. Björnsson and M. B. Green, 5 loops in 24/5 dimensions, J. High Energy Phys. 08 (2010) 132; J. Björnsson, Multiloop amplitudes in maximally supersymmetric pure spinor field theory, J. High Energy Phys. 01 (2011) 002.

[17] G. Bossard, P. S. Howe, K. S. Stelle, and P. Vanhove, The vanishing volume of $D = 4$ superspace, Classical Quantum Gravity **28**, 215005 (2011).

[18] Z. Bern, L. J. Dixon, D. C. Dunbar, M. Perelstein, and J. S. Rozowsky, On the relationship between Yang-Mills theory and gravity and its implication for ultraviolet divergences, Nucl. Phys. **B530**, 401 (1998).

[19] Z. Bern, J. J. Carrasco, L. J. Dixon, H. Johansson, D. A. Kosower, and R. Roiban, Three-Loop Superfiniteness of $N = 8$ Supergravity, Phys. Rev. Lett. **98**, 161303 (2007); Z. Bern, J. J. M. Carrasco, L. J. Dixon, H. Johansson, and R. Roiban, Manifest ultraviolet behavior for the three-loop four-point amplitude of $N = 8$ supergravity, Phys. Rev. D **78**, 105019 (2008); Z. Bern, J. J. Carrasco, L. J. Dixon, H. Johansson, and R. Roiban, Ultraviolet Behavior of $N = 8$

Supergravity at Four Loops, Phys. Rev. Lett. **103**, 081301 (2009).

[20] Z. Bern, J. J. M. Carrasco, L. J. Dixon, H. Johansson, and R. Roiban, Simplifying multiloop integrands and ultraviolet divergences of gauge theory and gravity amplitudes, Phys. Rev. D **85**, 105014 (2012).

[21] Z. Bern, J. J. M. Carrasco, L. J. Dixon, H. Johansson, and R. Roiban, Complete four-loop four-point amplitude in $N = 4$ super-Yang-Mills theory, Phys. Rev. D **82**, 125040 (2010).

[22] F. Gliozzi, J. Scherk, and D. I. Olive, Supersymmetry, supergravity theories and the dual spinor model, Nucl. Phys. **B122**, 253 (1977); L. Brink, J. H. Schwarz, and J. Scherk, Supersymmetric Yang-Mills theories, Nucl. Phys. **B121**, 77 (1977).

[23] S. Mandelstam, Light-cone Superspace and the finiteness of the $N = 4$ model, J. Phys. Colloq. **43**, C3-331 (1982); Light cone superspace and the ultraviolet finiteness of the $N = 4$ model, Nucl. Phys. **B213**, 149 (1983); L. Brink, O. Lindgren, and B. E. W. Nilsson, The ultraviolet finiteness of the $N = 4$ Yang-Mills theory, Phys. Lett. **123B**, 323 (1983); P. S. Howe, K. S. Stelle, and P. K. Townsend, The relaxed hypermultiplet: An unconstrained $N = 2$ superfield theory, Nucl. Phys. **B214**, 519 (1983).

[24] Z. Bern, S. Davies, and T. Dennen, Ultraviolet structure of half-maximal supergravity with matter multiplets at two and three loops, Phys. Rev. D **88**, 065007 (2013).

[25] Z. Bern, L. J. Dixon, D. C. Dunbar, and D. A. Kosower, One loop n-point gauge theory amplitudes, unitarity and collinear limits, Nucl. Phys. **B425**, 217 (1994); Fusing gauge theory tree amplitudes into loop amplitudes, Nucl. Phys. **B435**, 59 (1995); Z. Bern, L. J. Dixon, and D. A. Kosower, One loop amplitudes for e^+e^- to four partons, Nucl. Phys. **B513**, 3 (1998); R. Britto, F. Cachazo, and B. Feng, Generalized unitarity and one-loop amplitudes in $N = 4$ super-Yang-Mills, Nucl. Phys. **B725**, 275 (2005).

[26] Z. Bern, J. J. M. Carrasco, H. Johansson, and D. A. Kosower, Maximally supersymmetric planar Yang-Mills amplitudes at five loops, Phys. Rev. D **76**, 125020 (2007).

[27] Z. Bern, J. J. Carrasco, W. M. Chen, H. Johansson, and R. Roiban, Gravity Amplitudes as Generalized Double Copies of Gauge-Theory Amplitudes, Phys. Rev. Lett. **118**, 181602 (2017).

[28] Z. Bern, J. J. M. Carrasco, W. M. Chen, H. Johansson, R. Roiban, and M. Zeng, Five-loop four-point integrand of $N = 8$ supergravity as a generalized double copy, Phys. Rev. D **96**, 126012 (2017).

[29] H. Kawai, D. C. Lewellen, and S. H. H. Tye, A relation between tree amplitudes of closed and open strings, Nucl. Phys. **B269**, 1 (1986).

[30] Z. Bern, J. J. M. Carrasco, and H. Johansson, New relations for gauge-theory amplitudes, Phys. Rev. D **78**, 085011 (2008).

[31] Z. Bern, J. J. M. Carrasco, and H. Johansson, Perturbative Quantum Gravity as a Double Copy of Gauge Theory, Phys. Rev. Lett. **105**, 061602 (2010).

[32] Z. Bern, J. J. M. Carrasco, H. Johansson, and R. Roiban, Five-Loop Four-Point Amplitude of $N = 4$ Super-Yang-Mills Theory, Phys. Rev. Lett. **109**, 241602 (2012).

[33] See Supplemental Material at http://link.aps.org/supplemental/10.1103/PhysRevD.98.086021 for the N4YM_5loop.m file, which contains the improved super-Yang-Mills integrand, and the Level0Diagrams.m,…, Level6Diagrams.m files, which contain the improved super-gravity integrands.

[34] P. A. Baikov, K. G. Chetyrkin, and J. H. Kühn, Five-Loop Running of the QCD Coupling Constant, Phys. Rev. Lett. **118**, 082002 (2017); F. Herzog, B. Ruijl, T. Ueda, J. A. M. Vermaseren, and A. Vogt, The five-loop beta function of Yang-Mills theory with fermions, J. High Energy Phys. 02 (2007) 090; T. Luthe, A. Maier, P. Marquard, and Y. Schroder, Complete renormalization of QCD at five loops, J. High Energy Phys. 03 (2017) 020.

[35] K. G. Chetyrkin and F. V. Tkachov, Integration by parts: The algorithm to calculate beta functions in 4 loops, Nucl. Phys. **B192**, 159 (1981); Integration by parts: The algorithm to calculate beta functions in 4 loops, Nucl. Phys. **B192**, 159 (1981); S. Laporta, High precision calculation of multiloop Feynman integrals by difference equations, Int. J. Mod. Phys. A **15**, 5087 (2000); S. Laporta and E. Remiddi, The analytical value of the electron $(g-2)$ at order α^3 in QED, Phys. Lett. B **379**, 283 (1996); C. Anastasiou and A. Lazopoulos, Automatic integral reduction for higher order perturbative calculations, J. High Energy Phys. 07 (2004) 046; A. V. Smirnov, FIRE5: A C++ implementation of Feynman integral reduction, Comput. Phys. Commun. **189**, 182 (2015); A. von Manteuffel and C. Studerus, Reduze 2: Distributed Feynman integral reduction, arXiv:1201.4330; R. N. Lee, Presenting LiteRed: A tool for the loop integrals reduction, arXiv:1212.2685; B. Ruijl, T. Ueda, and J. A. M. Vermaseren, Forcer: A FORM program for the parametric reduction of four-loop massless propagator diagrams, arXiv:1704.06650; P. Maierhoefer, J. Usovitsch, and P. Uwer, Kira: A Feynman integral reduction program, Comput. Phys. Commun. **230**, 99 (2018).

[36] V. A. Smirnov, Analytic tools for Feynman integrals, Springer Tracts Mod. Phys. **250**, 1 (2012).

[37] J. Gluza, K. Kajda, and D. A. Kosower, Towards a basis for planar two-loop integrals, Phys. Rev. D **83**, 045012 (2011).

[38] D. A. Kosower and K. J. Larsen, Maximal unitarity at two loops, Phys. Rev. D **85**, 045017 (2012); S. Caron-Huot and K. J. Larsen, Uniqueness of two-loop master contours, J. High Energy Phys. 10 (2012) 026; M. Søgaard, Global residues and two-loop Hepta cuts, J. High Energy Phys. 09 (2013) 116; H. Johansson, D. A. Kosower, and K. J. Larsen, Maximal unitarity for the four-mass double box, Phys. Rev. D **89**, 125010 (2014); M. Søgaard and Y. Zhang, Multi-variate residues and maximal unitarity, J. High Energy Phys. 12 (2013) 008; Unitarity cuts of integrals with doubled propagators, J. High Energy Phys. 07 (2014) 112; S. Abreu, R. Britto, C. Duhr, and E. Gardi, Cuts from residues: The one-loop case, J. High Energy Phys. 06 (2017) 114.

[39] R. M. Schabinger, A new algorithm for the generation of unitarity-compatible integration by parts relations, J. High Energy Phys. 01 (2012) 077; H. Ita, Two-loop integrand decomposition into master integrals and surface terms, Phys. Rev. D **94**, 116015 (2016); K. J. Larsen and Y. Zhang, Integration-by-parts reductions from unitarity and algebraic geometry, Phys. Rev. D **93**, 041701 (2016); A. Georgoudis, K. J. Larsen, and Y. Zhang, Azurite: An algebraic geometry based package for finding bases of loop

integrals, Comput. Phys. Commun. **221,** 203 (2017); Z. Bern, M. Enciso, H. Ita, and M. Zeng, Dual conformal symmetry, integration-by-parts reduction, differential equations and the nonplanar sector, Phys. Rev. D **96,** 096017 (2017); D. A. Kosower, Direct solution of integration-by-parts systems, Phys. Rev. D **97,** 025008 (2018).

[40] Y. Zhang, Lecture notes on multiloop integral reduction and applied algebraic geometry, arXiv:1612.02249.

[41] G. Mogull and D. O'Connell, Overcoming obstacles to colour-kinematics duality at two loops, J. High Energy Phys. 12 (2015) 135.

[42] J. J. Carrasco and H. Johansson, Five-point amplitudes in $N = 4$ super-Yang-Mills theory and $N = 8$ supergravity, Phys. Rev. D **85,** 025006 (2012).

[43] Z. Bern, S. Davies, and J. Nohle, Double-copy constructions and unitarity cuts, Phys. Rev. D **93,** 105015 (2016).

[44] Z. Bern, T. Dennen, Y.-t. Huang, and M. Kiermaier, Gravity as the square of gauge theory, Phys. Rev. D **82,** 065003 (2010).

[45] M. Tolotti and S. Weinzierl, Construction of an effective Yang-Mills Lagrangian with manifest BCJ duality, J. High Energy Phys. 07 (2013) 111.

[46] M. Kiermaier, Amplitudes 2010, Queen Mary, University of London, http://www.strings.ph.qmul.ac.uk/theory/Amplitudes2010/Talks/MK2010.pdf; N. E. J. Bjerrum-Bohr, P. H. Damgaard, T. Sondergaard, and P. Vanhove, The momentum kernel of gauge and gravity theories, J. High Energy Phys. 01 (2011) 001; C. R. Mafra, O. Schlotterer, and S. Stieberger, Explicit BCJ numerators from pure spinors, J. High Energy Phys. 07 (2011) 092; Y. J. Du and C. H. Fu, Explicit BCJ numerators of nonlinear sigma model, J. High Energy Phys. 09 (2016) 174; N. E. J. Bjerrum-Bohr, J. L. Bourjaily, P. H. Damgaard, and B. Feng, Manifesting color-kinematics duality in the scattering equation formalism, J. High Energy Phys. 09 (2016) 094; Y. J. Du and F. Teng, BCJ numerators from reduced Pfaffian, J. High Energy Phys. 04 (2017) 033; Y. J. Du, B. Feng, and F. Teng, Expansion of all multitrace tree level EYM amplitudes, J. High Energy Phys. 12 (2017) 038.

[47] J. J. M. Carrasco and H. Johansson, Generic multiloop methods and application to $N = 4$ super-Yang-Mills, J. Phys. A **44,** 454004 (2011); J. J. M. Carrasco, Gauge and gravity amplitude relations, *Journeys Through the Precision Frontier: Amplitudes for Colliders TASI 2014, Proceedings of the 2014 Theoretical Advanced Study Institute in Elementary Particle Physics* (World Scientific, Singapore, 2015); M. Chiodaroli, Simplifying amplitudes in Maxwell-Einstein and Yang-Mills-Einstein supergravities, arXiv:1607.04129; C. Cheung, TASI lectures on scattering amplitudes, arXiv:1708.03872.

[48] Z. Bern, L. J. Dixon, M. Perelstein, and J. S. Rozowsky, Multileg one loop gravity amplitudes from gauge theory, Nucl. Phys. **B546,** 423 (1999).

[49] J. J. M. Carrasco, C. R. Mafra, and O. Schlotterer, Abelian Z-theory: NLSM amplitudes and α'-corrections from the open string, J. High Energy Phys. 06 (2017) 093.

[50] R. H. Boels, B. A. Kniehl, O. V. Tarasov, and G. Yang, Color-kinematic duality for form factors, J. High Energy Phys. 02 (2013) 063; Z. Bern, S. Davies, T. Dennen, Y.-t. Huang, and J. Nohle, Color-kinematics duality for

pure Yang-Mills and gravity at one and two loops, Phys. Rev. D **92,** 045041 (2015); C. R. Mafra and O. Schlotterer, Two-loop five-point amplitudes of super Yang-Mills and supergravity in pure spinor superspace, J. High Energy Phys. 10 (2015) 124; S. He, R. Monteiro, and O. Schlotterer, String-inspired BCJ numerators for one-loop MHV amplitudes, J. High Energy Phys. 01 (2016) 171; E. Herrmann and J. Trnka, Gravity on-shell diagrams, J. High Energy Phys. 11 (2016) 136; G. Yang, Color-Kinematics Duality and Sudakov Form Factor at Five Loops for $N = 4$ Super-symmetric Yang-Mills Theory, Phys. Rev. Lett. **117,** 271602 (2016); R. H. Boels, T. Huber, and G. Yang, Four-Loop Nonplanar Cusp Anomalous Dimension in $N = 4$ Super-symmetric Yang-Mills Theory, Phys. Rev. Lett. **119,** 201601 (2017); H. Johansson, G. Kälin, and G. Mogull, Two-loop supersymmetric QCD and half-maximal supergravity amplitudes, J. High Energy Phys. 09 (2017) 019.

[51] Z. Bern, S. Davies, and J. Nohle, Double-copy constructions and unitarity cuts, Phys. Rev. D **93,** 105015 (2016); G. Mogull and D. O'Connell, Overcoming obstacles to colour-kinematics duality at two loops, J. High Energy Phys. 12 (2015) 135.

[52] R. Monteiro, D. O'Connell, and C. D. White, Black holes and the double copy, J. High Energy Phys. 12 (2014) 056; A. Luna, R. Monteiro, D. O'Connell, and C. D. White, The classical double copy for Taub-NUT spacetime, Phys. Lett. B **750,** 272 (2015); G. Cardoso, S. Nagy, and S. Nampuri, Multi-centered $\mathcal{N} = 2$ BPS black holes: A double copy description, J. High Energy Phys. 04 (2017) 037; T. Adamo, E. Casali, L. Mason, and S. Nekovar, Scattering on plane waves and the double copy, Classical Quantum Gravity **35,** 015004 (2018); N. Bahjat-Abbas, A. Luna, and C. D. White, The Kerr-Schild double copy in curved spacetime, J. High Energy Phys. 12 (2017) 004; M. Carrillo-González, R. Penco, and M. Trodden, The classical double copy in maximally symmetric spacetimes, J. High Energy Phys. 04 (2018) 028.

[53] A. Luna, R. Monteiro, I. Nicholson, D. O'Connell, and C. D. White, The double copy: Bremsstrahlung and accelerating black holes, J. High Energy Phys. 06 (2016) 023; W. D. Goldberger and A. K. Ridgway, Radiation and the classical double copy for color charges, Phys. Rev. D **95,** 125010 (2017); A. Luna, R. Monteiro, I. Nicholson, A. Ochirov, D. O'Connell, N. Westerberg, and C. D. White, Perturbative spacetimes from Yang–Mills theory, J. High Energy Phys. 04 (2017) 069; W. D. Goldberger, S. G. Prabhu, and J. O. Thompson, Classical gluon and graviton radiation from the bi-adjoint scalar double copy, Phys. Rev. D **96,** 065009 (2017); W. D. Goldberger, J. Li, and S. G. Prabhu, Spinning particles, axion radiation, and the classical double copy, Phys. Rev. D **97,** 105018 (2018); W. D. Goldberger and A. K. Ridgway, Bound states and the classical double copy, Phys. Rev. D **97,** 085019 (2018); J. Li and S. G. Prabhu, Gravitational radiation from the classical spinning double copy, Phys. Rev. D **97,** 105019 (2018).

[54] N. E. J. Bjerrum-Bohr, J. F. Donoghue, B. R. Holstein, L. Plantè, and P. Vanhove, Bending of Light in Quantum Gravity, Phys. Rev. Lett. **114,** 061301 (2015); Light-like scattering in quantum gravity, J. High Energy Phys. 11 (2016) 117; N. E. J. Bjerrum-Bohr, B. R. Holstein, J. F.

Donoghue, L. Planté, and P. Vanhove, Illuminating light bending, Proc. Sci., CORFU 2016 (**2017**) 077 [arXiv: 1704.01624].

[55] L. Borsten, M. J. Duff, L. J. Hughes, and S. Nagy, Magic Square from Yang-Mills Squared, Phys. Rev. Lett. **112,** 131601 (2014); A. Anastasiou, L. Borsten, M. J. Duff, L. J. Hughes, and S. Nagy, A magic pyramid of supergravities, J. High Energy Phys. 04 (2014) 178; Yang-Mills Origin of Gravitational Symmetries, Phys. Rev. Lett. **113,** 231606 (2014).

[56] J. J. M. Carrasco, M. Chiodaroli, M. Gunaydin, and R. Roiban, One-loop four-point amplitudes in pure and matter-coupled $N \leq 4$ supergravity, J. High Energy Phys. 03 (2013) 056; M. Chiodaroli, M. Gunaydin, H. Johansson, and R. Roiban, Scattering amplitudes in $\mathcal{N} = 2$ Maxwell-Einstein and Yang–Mills-Einstein supergravity, J. High Energy Phys. 01 (2015) 081; Explicit formulae for Yang-Mills-Einstein amplitudes from the double copy, J. High Energy Phys. 07 (2017) 002.

[57] M. Chiodaroli, M. Gunaydin, H. Johansson, and R. Roiban, Spontaneously broken Yang-Mills-Einstein supergravities as double copies, J. High Energy Phys. 06 (2017) 064; Complete Construction of Magical, Symmetric and Homogeneous $N = 2$ Supergravities as Double Copies of Gauge Theories, Phys. Rev. Lett. **117,** 011603 (2016); A. Anastasiou, L. Borsten, M. J. Duff, M. J. Hughes, A. Marrani, S. Nagy, and M. Zoccali, Twin supergravities from Yang-Mills theory squared, Phys. Rev. D **96,** 026013 (2017); A. Anastasiou, L. Borsten, M. J. Duff, A. Marrani, S. Nagy, and M. Zoccali, Are all supergravity theories Yang-Mills squared?, arXiv:1707.03234; M. Chiodaroli, M. Gunaydin, H. Johansson, and R. Roiban, Gauged supergravities and spontaneous SUSY breaking from the double copy, arXiv:1710.08796.

[58] T. Bargheer, S. He, and T. McLoughlin, New Relations for Three-Dimensional Supersymmetric Scattering Amplitudes, Phys. Rev. Lett. **108,** 231601 (2012); Y.-t. Huang and H. Johansson, Equivalent $D = 3$ Supergravity Amplitudes from Double Copies of Three-Algebra and Two-Algebra Gauge Theories, Phys. Rev. Lett. **110,** 171601 (2013); Y.-t. Huang, H. Johansson, and S. Lee, On three-algebra and bi-fundamental matter amplitudes and integrability of supergravity, J. High Energy Phys. 11 (2013) 050.

[59] G. Chen and Y. J. Du, Amplitude relations in non-linear sigma model, J. High Energy Phys. 01 (2014) 061; F. Cachazo, S. He, and E. Y. Yuan, Scattering equations and matrices: From Einstein To Yang-Mills, DBI and NLSM, J. High Energy Phys. 07 (2015) 149; F. Cachazo, P. Cha, and S. Mizera, Extensions of theories from soft limits, J. High Energy Phys. 06 (2016) 170; C. R. Mafra and O. Schlotterer, Non-Abelian Z-theory: Berends-Giele recursion for the α'-expansion of disk integrals, J. High Energy Phys. 01 (2017) 031; J. J. M. Carrasco, C. R. Mafra, and O. Schlotterer, Semi-Abelian Z-theory: NLSM $+ \phi^3$ from the open string, J. High Energy Phys. 08 (2017) 135; C. Cheung, C. H. Shen, and C. Wen, Unifying relations for scattering amplitudes, J. High Energy Phys. 02 (2018) 095.

[60] C. Cheung and C. H. Shen, Symmetry for Flavor-Kinematics Duality from an Action, Phys. Rev. Lett. **118,** 121601 (2017).

[61] J. Broedel, O. Schlotterer, and S. Stieberger, Polylogarithms, Multiple zeta values and superstring amplitudes, Fortsch. Phys. **61,** 812 (2013); S. Stieberger and T. R. Taylor, Closed string amplitudes as single-valued open string amplitudes, Nucl. Phys. **B881,** 269 (2014); Y.-t. Huang, O. Schlotterer, and C. Wen, Universality in string interactions, J. High Energy Phys. 09 (2016) 155; C. R. Mafra and O. Schlotterer, The Double-Copy Structure of One-Loop Open-String Amplitudes, Phys. Rev. Lett. **120,** 011601 (2018); T. Azevedo, M. Chiodaroli, H. Johansson, and O. Schlotterer, Heterotic and bosonic string amplitudes via field theory, arXiv:1803.05452.

[62] H. Johansson and J. Nohle, Conformal gravity from gauge theory, arXiv:1707.02965.

[63] H. Johansson and A. Ochirov, Pure gravities via color-kinematics duality for fundamental matter, J. High Energy Phys. 11 (2015) 046; Color-kinematics duality for QCD amplitudes, J. High Energy Phys. 01 (2016) 170.

[64] V. P. Nair, A current algebra for some gauge theory amplitudes, Phys. Lett. B **214,** 215 (1988).

[65] H. Elvang, D. Z. Freedman, and M. Kiermaier, Recursion relations, generating functions, and unitarity sums in $N = 4$ SYM Theory, J. High Energy Phys. 04 (2009) 009; Z. Bern, J. J. M. Carrasco, H. Ita, H. Johansson, and R. Roiban, Structure of supersymmetric sums in multiloop unitarity cuts, Phys. Rev. D **80,** 065029 (2009).

[66] C. Cheung and D. O'Connell, Amplitudes and spinor-helicity in six dimensions, J. High Energy Phys. 07 (2009) 075; T. Dennen, Y.-t. Huang, and W. Siegel, Super-twistor space for 6D maximal super Yang-Mills, J. High Energy Phys. 04 (2010) 127; Z. Bern, J. J. Carrasco, T. Dennen, Y.-t. Huang, and H. Ita, Generalized unitarity and six-dimensional helicity, Phys. Rev. D **83,** 085022 (2011).

[67] S. H. Henry Tye and Y. Zhang, Dual identities inside the gluon and the graviton scattering amplitudes, J. High Energy Phys. 06 (2010) 071; Erratum: Dual identities inside the gluon and the graviton scattering amplitudes, J. High Energy Phys. 04 (2011) 114; N. E. J. Bjerrum-Bohr, P. H. Damgaard, T. Sondergaard, and P. Vanhove, Monodromy and Jacobi-like relations for color-ordered amplitudes, J. High Energy Phys. 06 (2010) 003.

[68] Z. Bern, J. S. Rozowsky, and B. Yan, Two loop four gluon amplitudes in $N = 4$ superYang-Mills, Phys. Lett. B **401,** 273 (1997).

[69] A. A. Vladimirov, Method for computing renormalization group functions in dimensional renormalization scheme, Teor. Mat. Fiz. **43,** 210 (1980) [Theor. Math. Phys. **43,** 417 (1980)]; N. Marcus and A. Sagnotti, A simple method for calculating counterterms, Nuovo Cim. A **87,** 1 (1985); M. Beneke and V. A. Smirnov, Asymptotic expansion of Feynman integrals near threshold, Nucl. Phys. **B522,** 321 (1998).

[70] T. Luthe, Fully massive vacuum integrals at 5 loops, Ph.D. thesis, Bielefeld University, 2015.

[71] A. Pak, The toolbox of modern multi-loop calculations: Novel analytic and semi-analytic techniques, J. Phys. Conf. Ser. **368,** 012049 (2012).

[72] J. Hoff, The Mathematica package TopoID and its application to the Higgs boson production cross section, J. Phys. Conf. Ser. **762,** 012061 (2016).

[73] A. Primo and L. Tancredi, On the maximal cut of Feynman integrals and the solution of their differential equations, Nucl. Phys. **B916**, 94 (2017); H. Frellesvig and C. G. Papadopoulos, Cuts of Feynman Integrals in Baikov representation, J. High Energy Phys. 04 (2017) 083; J. Bosma, M. Søgaard, and Y. Zhang, Maximal cuts in arbitrary dimension, J. High Energy Phys. 08 (2017) 051; A. Primo and L. Tancredi, Maximal and differential equations for Feynman integrals. An application to the three-loop massive banana graph, Nucl. Phys. **B921**, 316 (2017); M. Harley, F. Moriello, and R. M. Schabinger, Baikov-Lee representations of cut Feynman integrals, J. High Energy Phys. 06 (2017) 049.

[74] S. Abreu, F. Febres Cordero, H. Ita, M. Jaquier, B. Page, and M. Zeng, Two-Loop Four-Gluon Amplitudes with the Numerical Unitarity Method, Phys. Rev. Lett. **119**, 142001 (2017); S. Abreu, F. Febres Cordero, H. Ita, B. Page, and M. Zeng, Planar Two-loop five-gluon amplitudes from numerical unitarity, arXiv:1712.03946.

[75] M. Søgaard and Y. Zhang, Unitarity cuts of integrals with doubled propagators, J. High Energy Phys. 07 (2014) 112; H. Johansson, D. A. Kosower, K. J. Larsen, and M. Søgaard, Cross-order integral relations from maximal cuts, Phys. Rev. D **92**, 025015 (2015); G. Chen, J. Liu, R. Xie, H. Zhang, and Y. Zhou, Syzygies probing scattering amplitudes, J. High Energy Phys. 09 (2016) 075.

[76] Z. Bern, L. J. Dixon, and D. A. Kosower, Dimensionally regulated one loop integrals, Phys. Lett. B **302**, 299 (1993); Erratum: Dimensionally regulated one loop integrals, Phys. Lett. B **318**, 649 (1993); O. V. Tarasov, Connection between Feynman integrals having different values of the space-time dimension, Phys. Rev. D **54**, 6479 (1996).

[77] W. Decker, G.-M. Greuel, G. Pfister, and H. Schönemann, Singular 4-1-1: A computer algebra system for polynomial computations, http://www.singular.uni-kl.de, 2018.

[78] P. A. Baikov, Explicit solutions of the three loop vacuum integral recurrence relations, Phys. Lett. B **385**, 404 (1996); Explicit solutions of the multiloop integral recurrence relations and its application, Nucl. Instrum. Methods Phys. Res., Sect. A **389**, 347 (1997); R. E. Cutkosky, Singularities and discontinuities of Feynman amplitudes, J. Math. Phys. **1**, 429 (1960); A. G. Grozin, Integration by parts: An introduction, Int. J. Mod. Phys. A **26**, 2807 (2011).

[79] A. von Manteuffel and R. M. Schabinger, A novel approach to integration by parts reduction, Phys. Lett. B **744**, 101 (2015); T. Peraro, Scattering amplitudes over finite fields and multivariate functional reconstruction, J. High Energy Phys. 12 (2016) 030.

[80] J.-G. Dumas, T. Gautier, M. Giesbrecht, P. Giorgi, B. Hovinen, E. Kaltofen, B. D. Saunders, W. J. Turner, and G. Villard, LinBox: A generic library for exact linear algebra, Mathematical Software, July 2002, pp. 40–50, http://www.linalg.org.

[81] A. von Manteuffel and R. M. Schabinger, Quark and gluon form factors to four-loop order in QCD: the N_f^3 contributions, Phys. Rev. D **95**, 034030 (2017).

[82] A. V. Smirnov and M. N. Tentyukov, Feynman integral evaluation by a sector decomposiTion approach (FIESTA), Comput. Phys. Commun. **180**, 735 (2009); A. V. Smirnov, V. A. Smirnov, and M. Tentyukov, FIESTA 2: Parallelizeable multiloop numerical calculations, Comput. Phys. Commun. **182**, 790 (2011); A. V. Smirnov, FIESTA 3: Cluster-parallelizable multiloop numerical calculations in physical regions, Comput. Phys. Commun. **185**, 2090 (2014).

[83] Z. Bern, J. J. Carrasco, L. J. Dixon, M. R. Douglas, M. von Hippel, and H. Johansson, $D = 5$ maximally supersymmetric Yang–Mills theory diverges at six loops, Phys. Rev. D **87**, 025018 (2013).

[84] Z. Bern, N. E. J. Bjerrum-Bohr, and D. C. Dunbar, Inherited twistor-space structure of gravity loop amplitudes, J. High Energy Phys. 05 (2005) 056; N. E. J. Bjerrum-Bohr and P. Vanhove, Explicit cancellation of triangles in one-loop gravity amplitudes, J. High Energy Phys. 04 (2008) 065; Absence of triangles in maximal supergravity amplitudes, J. High Energy Phys. 10 (2008) 006; N. Arkani-Hamed, F. Cachazo, and J. Kaplan, What is the simplest quantum field theory?, J. High Energy Phys. 09 (2010) 016.